博士論文

Relationship between Mitral Leaflet Size and Coaptation-zone area and their Associated Factors in Patients with Normal Left Ventricular Size and Systolic Function : Real-time 3D Echocardiographic Analysis

（僧帽弁の弁葉面積と接合面積に影響する臨床因子とは －リアルタイム３次元心エコー図による解析）

徐　博卿

Xu Boqing

Relationship between Mitral Leaflet Size and Coaptation-zone area and their Associated Factors in Patients with Normal Left Ventricular Size and Systolic Function: Real-time 3D Echocardiographic Analysis

The University of Tokyo Graduate School of Medicine

Research supervisor: Professor Yutaka Yatomi

Boqing Xu

Contents

	Pages
Abbreviations	**4**
Abstract	**5 - 6**
Introduction	**7 - 15**
Step 1 study	
Aims and Methods	**16 - 28**
Results	**29 - 41**
Step 2 study	
Aims and Methods	**42 - 46**
Results	**47 - 53**
Discussion	**54 - 64**
Acknowledgments	**65**
References	**66 - 78**

Abbreviations

AP/ M-L	**Anterior-posterior/ medial-lateral**
AS	**Aortic stenosis**
BSA	**Body surface area**
BMI	**Body mass index**
BP	**Blood pressure**
CAD	**Coronary artery disease**
CAVI	**Cardio-ankle vascular index**
CKD	**Chronic kidney disease**
FMR	**Functional mitral regurgitation**
HDL/ LDL	**High-density lipoprotein/ low-density lipoprotein**
HF	**Heart failure**
IVST	**Interventricular septal wall thickness**
LA / LV	**Left atrium/atrial/left ventricle/ventricular**
LVEDV/LVESV	**Left ventricular end-diastolic and end-systolic volume**
LVDD	**Left ventricular diastolic diameter**
LVID	**Left ventricular internal diameter**
MV	**Mitral valve/valvular**
PWT	**Posterior wall thickness**
RT3DE	**Real-time 3D echocardiography**

Abstract

Functional mitral regurgitation (FMR) is a complication in patients with ischemic and dilated cardiomyopathy, and is associated with poor clinical outcome. Recently, enlargement of the mitral valve (MV) has gained attention as a compensatory mechanism for FMR. I aimed to elucidate the clinical factors that are associated with reduced MV leaflet area and coaptation-zone area using real-time 3D echocardiography (RT3DE).

This study had two steps. The first step was to find which clinical factors were associated with MV in 175 patients with normal left ventricle (LV) size and ejection fraction. There was a significant relationship between the MV leaflet area and the coaptation-zone area ($r=0.481$, $p<0.001$). MV leaflet area was strongly and positively associated with body surface area (BSA) ($r=0.907$, $p<0.001$). MV leaflet area/BSA was independently associated with diastolic blood pressure ($p<0.001$) and LV end-diastolic volume (LVEDV) index ($p<0.001$). Both MV coaptation-zone area/BSA and MV coaptation-zone area/MV leaflet area were positively and independently associated with LVEDV index ($p=0.001$, $p=0.003$). MV coaptation-zone area/MV leaflet area was negatively and independently associated with coronary artery disease (CAD) ($p=0.034$)

The second step was to determine if MV leaflet and coaptation-zone areas were associated with atherosclerosis assessed by cardio-ankle vascular index (CAVI) in 66 patients with normal LV size and ejection fraction. CAVI is a blood pressure-independent parameter of arterial stiffness. In multivariable analysis, mean CAVI was independently associated with MV leaflet area/BSA ($r = -0.440$, $p = 0.015$) and with MV coaptation-zone area/BSA ($r = -0.611$, $p < 0.001$), and with MV coaptation-zone area/MV leaflet area ($r = -0.530$, $p < 0.001$).

In conclusion, the MV leaflet area might be intrinsically determined by body size. On the other hand, some clinical factors associated with atherosclerosis might also influence MV leaflet and coaptation-zone areas, which are associated with the generation of FMR.

Introduction

Functional mitral regurgitation (FMR), also known as secondary mitral regurgitation (MR), is caused by geometrical abnormalities of the subvalvular mitral complex (Figure 1) and is a common complication in patients with non-ischemic or ischemic cardiomyopathy even in the absence of structural abnormalities of the mitral valve (MV) (Figure 2). FMR elicits left ventricular (LV) volume overload by regurgitation, leading to progressive myocardial dysfunction associated with poor clinical outcome over the world [1, 2].

In a patient with heart failure (HF), the complication of FMR is a critical factor underlying the poor clinical outcome [3]. Continuous LV overload by FMR progresses to LV systolic dysfunction and LV remodeling, resulting in further deterioration of MV tethering and FMR [4]. LV systolic dysfunction also increases cardiac preload and decreases cardiac afterload, decreasing the force of pressure differential strength of MV leaflet coaptation, in turn causing dynamic FMR [5–8]. As all the above pathological factors develop continuously, FMR is associated with a poor prognosis in patients with HF. In HF complicated with FMR (Figure 3), the prognosis is poor during treatment whether or not the LV ejection fraction becomes normal, because cardiac preload and LV ventricular

volume overload are still higher in HF with FMR than without it.

Figure 1. Pathophysiology of functional mitral regurgitation in dilated or ischemic cardiomyopathy.

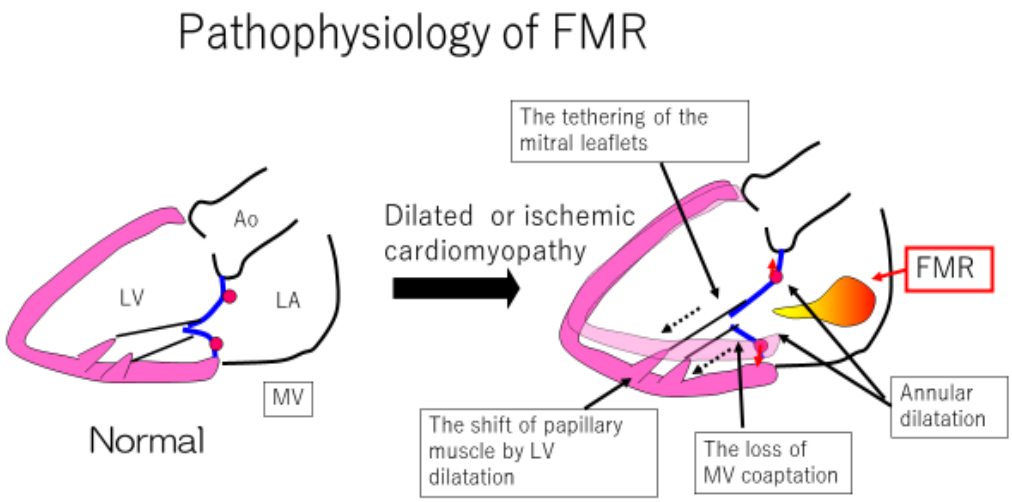

Produced by Boqing Xu

In dilated cardiomyopathy or ischemic cardiomyopathy with FMR, the distance between papillary muscles (shifted into posterior and lateral displacement) and MV leaflets is increased passively. At the same time, because the length of chordae tendineae remain constant, becoming insufficient to connect the passively displaced papillary muscles and MV leaflets, this elicits tethering of the mitral leaflets, and inappropriate leaflet coaptation, resulting in regurgitation.

Ao, aorta. LA, left atrium. LV, left ventricle. MV, mitral valve. FMR, functional mitral regurgitation.

Figure 2. Non-ischemic cardiomyopathy complicated by function mitral regurgitation

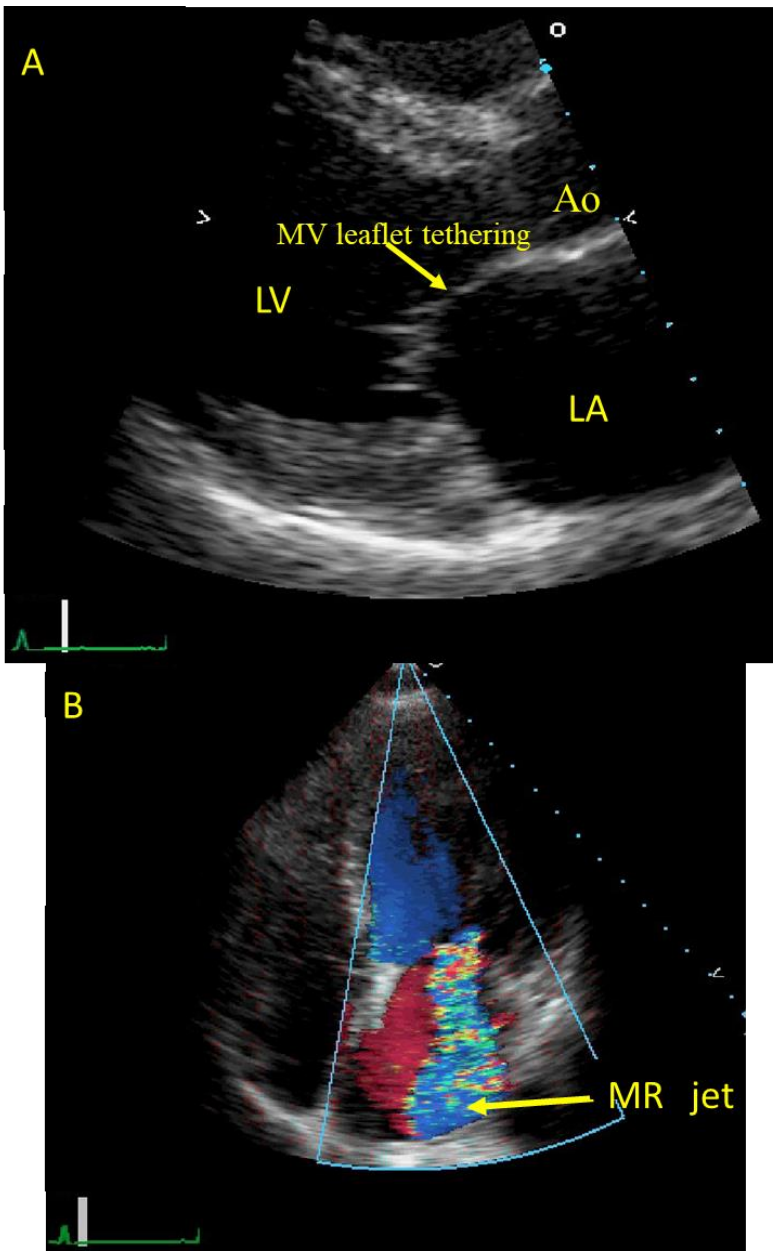

Figure 2A. Echocardiography shows that the MV leaflets were tethered to the apical direction in mid systole resulting in the loss of valve coaptation in a patient with dilated cardiomyopathy.

Figure 2B. Color Doppler image shows a central jet of FMR caused by MV tethering with LV dilatation.

Ao, aorta. LA, left atria. LV, left ventricle. MV, mitral valve. MR, mitral regurgitation. FMR, functional mitral regurgitation.

Figure 3. Left ventricular pressure-volume curve in heart failure complicated by FMR and without FMR.

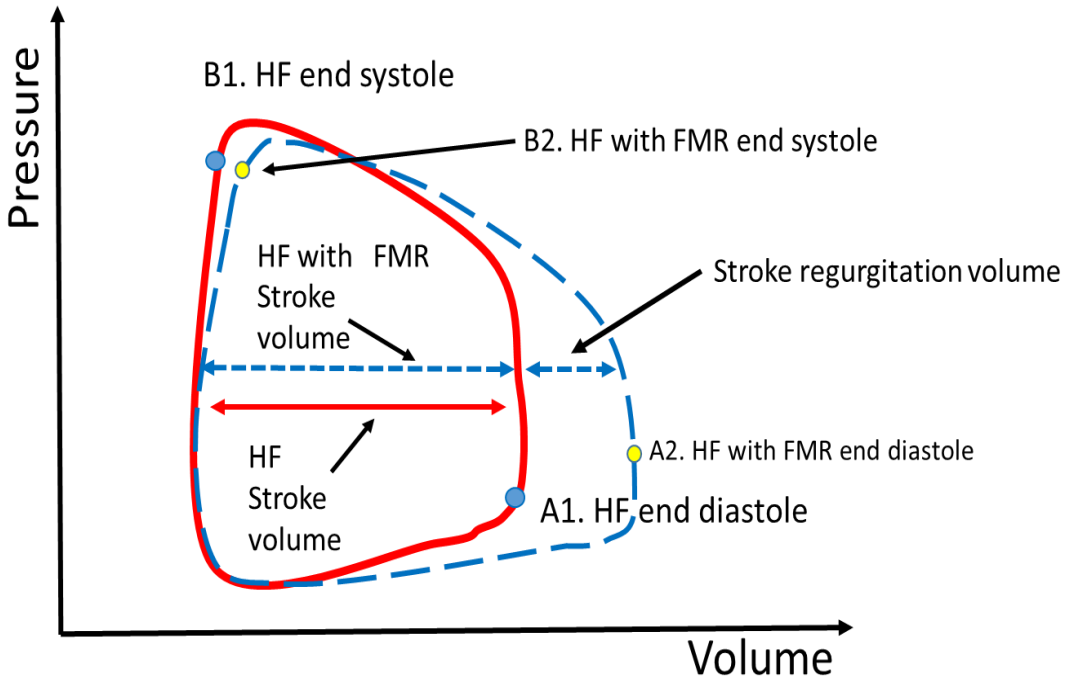

Produced by Boqing Xu

In heart failure with FMR, the curve in end-diastole, the left ventricle suffers from volume overload compared with non-FMR. But at the end of systole, the stroke volume in FMR heart failure is much smaller than in a non-FMR one. This pathological process leads to poor clinical outcomes.

HF, heart failure. FMR, functional mitral regurgitation.

FMR is also known to be associated with poor clinical outcomes in patients with atrial fibrillation (AF) [9]. The dilated left atrium (LA) pushes the crest of the LV inlet against the posterior MV leaflet, and the MV annular plane is displaced in the superior direction, causing atriogenic MV leaflet tethering [10–15]. AF complicated by FMR becomes increasingly important because 9% AF (1-10 years) and 29% AF (>10 years) have FMR with poor clinical outcome [11, 16]. Furthermore, FMR is also associated with a poor outcome in ischemic cardiac disease [17, 18]. Thus, FMR accounted for one-fifth of complications due to acute myocardial infarction and half of those who suffered from congestive heart failure [19]. The pathology is that ischemic remodeling of the LV causes displacement of papillary muscles and changes the MV leaflet adaptation (enlargement and stiffness [19]), resulting in tethering of the leaflets and reducing their coaptation [20].

FMR is expected to increase further in the near future with the growing number of HF patients [21]. Therefore, it is critical to understand the pathophysiology of FMR and to establish preventive and therapeutic strategies for the condition.

There is considerable evidence from animal experiments and clinical studies [22, 23]

that the tethering of the MV leaflets by a dilated LV and papillary muscle displacement plays a central role in the generation of FMR (Figure 1) [24]. The leaflets of the MV remain closed during the systolic phase of the LV with the help of papillary muscle contraction and the chordae tendineae connecting them normally. In a dilated LV, the distance between the papillary muscles and MV leaflets is increased passively, whereas the length of chordae tendineae remains constant [1]. These geometrical abnormalities of the mitral complex lead to a shift of the mitral tips in the apical direction, resulting in malcoaptation of the MV leaflets and generation of FMR. LV dilation also may cause mitral annular dilation, which is also postulated to contribute to the progression of FMR [25, 26].

Recently, MV leaflet size has gained attention as a possible underlying mechanism of progression of FMR, because the size of the MV leaflets is an essential component of the closure of the valve [19, 23, 27, 28]. MV leaflets are dynamic and influenced by multiple factors [29]. In patients with a dilated LV, the mitral leaflets may be elongated due to stress imposed by tethering, and mitral leaflet elongation due to tethering may compensate for a reduced MV coaptation-zone area. However, as some patients have FMR without significant LV dilation, such as those with degenerative aortic stenosis

(AS) [30–33], it has been suggested that atherosclerosis-related risk factors might influence the mitral leaflet degeneration [34], presenting with a reduced size and hindering compensatory mitral leaflet elongation. It has been reported that compensatory and intrinsic metabolism occurs within the MV leaflet, named endothelial-mesenchymal trans-differentiation capacity and that this capacity actively enlarges the size of the MV leaflet area through a complex embryonic developmental pathway in the leaflet tissue [35, 36].

According to the above, it has been hypothesized that atherosclerosis-related risk factors may be associated with MV leaflet size and coaptation. Real-time 3D echocardiography allows quantitative measurements of the MV leaflet area and subvalvular apparatus with 3D software (Figure 4). To address this hypothesis, I planned a two-step study using RT3DE in patients with normal LV size and function, where the MV tethering did not influence the MV leaflet size and coaptation. The first study was to find which clinical factors were associated with MV in patients with normal LV size and ejection fraction. The second study was aimed to determine if the MV leaflet and coaptation-zone areas were associated with the severity of atherosclerosis as assessed by the cardio-ankle vascular index (CAVI).

Figure 4. Reconstruction of the mitral complex by real-time 3D echocardiography.

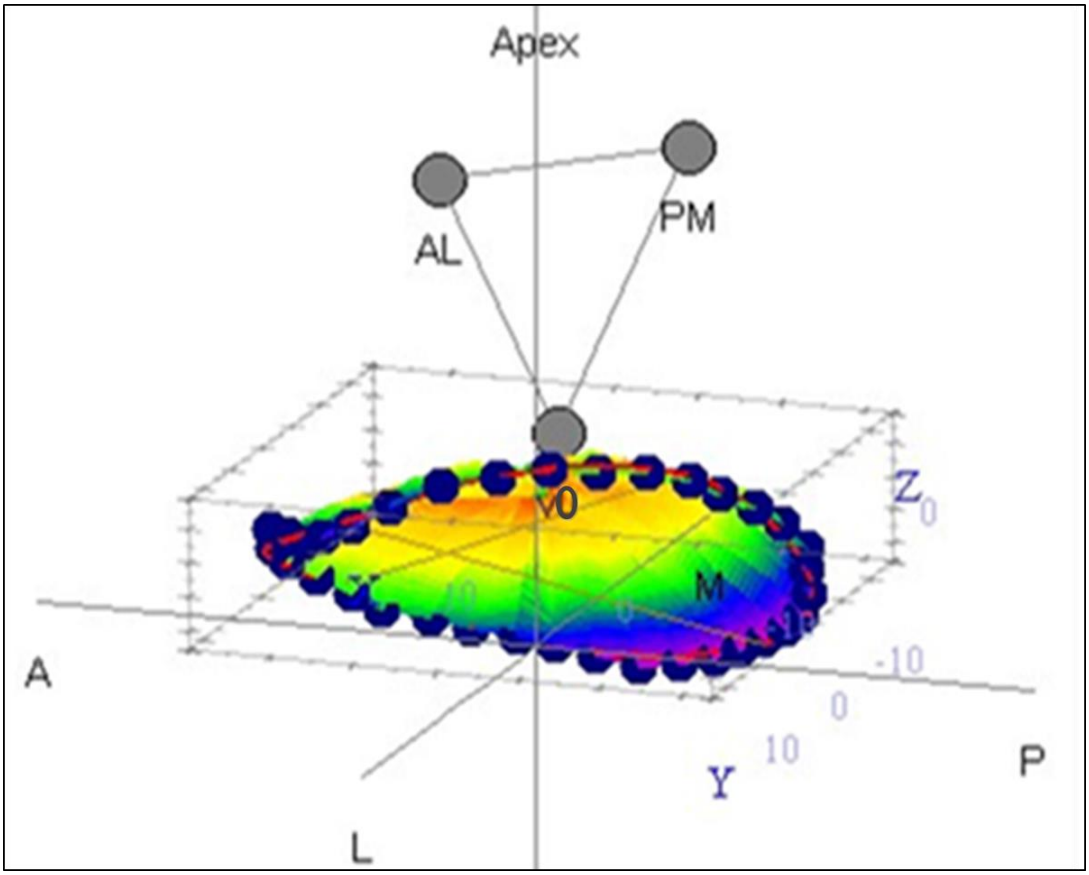

Mitral valvular (MV) leaflets can be reconstructed by 3D software (Realview^{TM}) using real-time 3D echocardiographic images. It allows 3-dimensional measurements of the mitral complex including the MV leaflet area. The blue ball represents the MV annulus. The color area enclosed inside the MV annulus represents the MV leaflet area for measuring at the time of the onset of MV closure. The color area enclosed inside the MV annulus, when measured in the time of mid-systole, represents the MV base-clear-zone area. A, anterior. AL, anterior-lateral papillary muscle. L, lateral. M, medium. P, posterior. PM, posterior-medium papillary muscle. V0, the endpoint of the maximum tenting length in coaptation. Y, y-axis. Z, z-axis.

Step 1 study

Aims

I aimed to determine if the MV leaflet area is associated with the MV coaptation-zone area and to identify the clinical factors associated with MV leaflet size and coaptation-zone area in patients with normal LV systolic function and LV size using RT3DE.

Methods

1. Study subjects

3D echocardiographic volume data were obtained in consecutive subjects who underwent conventional echocardiography using iE33 (Philips, Andover, MA, USA) for screening or assessing heart disease, from 8 October 2015 to 31 December 2017 at the University of Tokyo Hospital. Out of the pooled 3D data set, I screened my study subjects according to 2D echocardiographic screening criteria and added retrospective 3D echocardiographic analysis.

My 2D echocardiographic screening criteria were normal LV dimension (an indexed LV end-diastolic diameter < 3.3 cm/m^2) [37] and normal systolic function (LV ejection fraction ≥ 50%) without regional LV wall motion abnormalities in mixed clinical conditions. The study enrolled 386 patients with normal LV dimensions and ejection

fraction. I excluded patients with cardiomyopathy, atrial fibrillation, and significant valvular heart disease except for FMR in which MV was structurally normal, as all might influence mitral leaflet size [19, 23, 27, 28]. Patients with atrial fibrillation were excluded from this study for an inadequate forming 3D echocardiographic image due to irregular heart rates. This is because the whole 3D volume data of the mitral complex requires combined 3D images of 4 heartbeats at the same interval. Furthermore, based on a previous study that reported normal values of 3D echocardiographic measurements and their gender differences, I finally enrolled only cases who had normal LV size by 3D echocardiographic measurements (LV end-diastolic volume index of 26~74 ml/m^2 for males, and 28~64 ml/m^2 for females) [38]. I collected clinical data on each patient at the time of the first visit to the hospital and during the follow-up period from medical records. I also determined if patients had hypertension, diabetes, dyslipidemia, coronary artery disease (CAD), chronic kidney disease (CKD), ischemic stroke, or a regular smoking habit and if they were on hemodialysis. Hypertension was defined as systolic blood pressure (BP) ≥140 mmHg or a diastolic BP ≥90 mmHg, measured repeatedly, or the use of antihypertensive therapy. Diabetes mellitus was defined as an overnight fasting serum glucose ≥126 mg/dL on at least two separate occasions or treatment with antidiabetic therapy. Dyslipidemia was defined as a serum level of total cholesterol

≥220 mg/dL, triglycerides ≥150 mg/dL, low-density lipoprotein (LDL) cholesterol ≥140 mg/dL, or high-density lipoprotein (HDL) cholesterol <40 mg/dL, or the use of lipid-lowering therapy. The presence of CAD was defined as a history of CAD, which was previously established if a major coronary artery had >50% diameter stenosis based on coronary angiography or computed tomography. CKD was defined as a gradual loss of renal function over time that progressed to 2nd stage CKD (eGFR 60-90ml/min/1.73m^2) or more severe stages. Ischemic stroke was diagnosed based on the findings of magnetic resonance imaging. This cross-sectional study was approved by the institutional ethics committee of the University of Tokyo (# 2650), and the requirement for informed consent was waived because I used de-identified data routinely collected during daily practice.

2. Conventional echocardiography

Conventional echocardiography was performed consecutively in a prospective fashion. Two-dimensional and color Doppler imaging was performed to screen for valvular stenosis or regurgitation. LV mass and left atrial (LA) volume index were measured by 2-dimensional echocardiography, according to published guidelines [37]. I used the cube formula to calculate LV mass during the end-diastolic period: LV mass (g) = 0.8 × 1.04× [(IVST + LVID + PWT)^3 - LVID^3] + 0.6 (g) (IVST, interventricular septal wall

thickness; LVID, LV internal diameter; PWT, posterior wall thickness.) [37]. LV mass index was calculated as LV mass/ body surface area (BSA). LA volume was measured using the biplane area-length method [37]. LA volume index was calculated as LA volume/BSA. I obtained transmitral diastolic flow by pulsed-wave Doppler from the apical four-chamber view (Figure 5). Peak velocities of the early (E-wave) and late (A-wave) phases of the mitral inflow pattern from Doppler recordings were measured in the apical four-chamber view, and their ratio (E/A) was calculated. The peak early diastolic (e') velocity of the septal mitral annulus was measured by pulsed tissue Doppler imaging in the apical four-chamber view. The ratio of the E-wave to the e' velocity (E/e') was calculated as an index of LV filling pressure [39]. The severity of MR was graded semi-quantitatively by color Doppler studies of the spatial distribution of the regurgitate jet [40]. The echocardiographic machines and laboratory are maintained under the guidelines of the Japanese Society of Echocardiography [41].

Figure 5. Mitral inflow pattern in echocardiography.

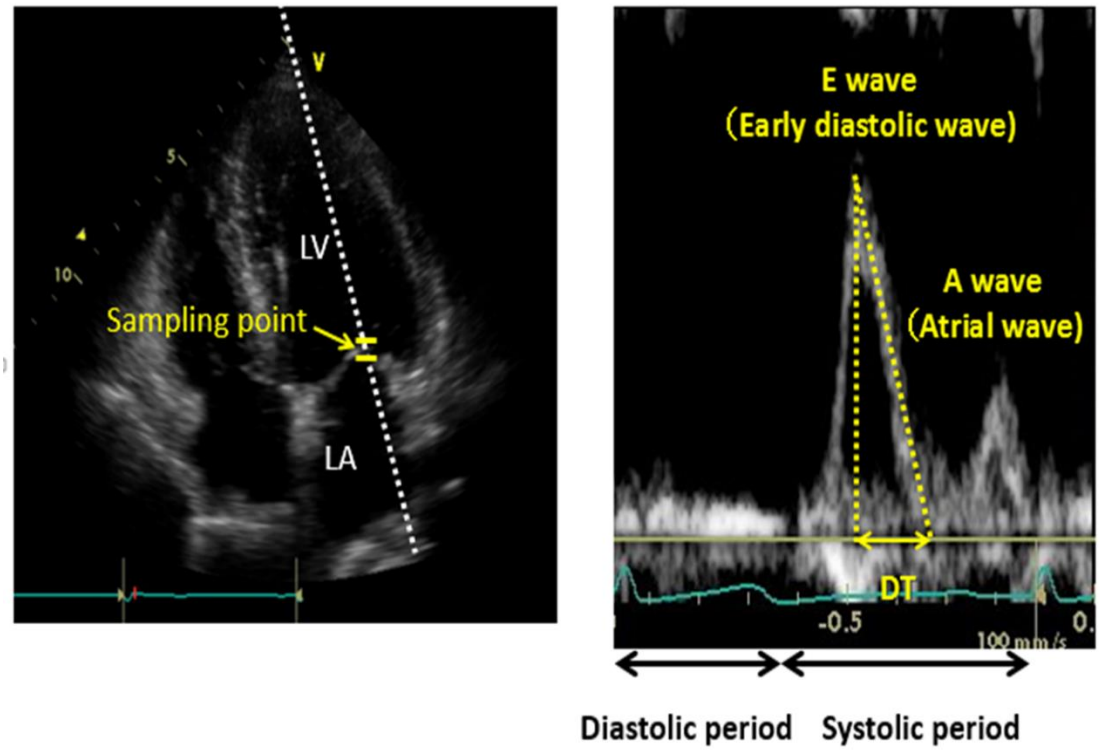

The sampling point of pulsed-wave Doppler was - at the point of mitral closure in the apical windows (left). Normal mitral inflow showed a predominant E-wave at early diastole, and a small A-wave at late diastole (right). DT, deceleration time. LA, left atria. LV, left ventricle.

3. 3D echocardiographic data acquisition and LV volume measurements

An iE33xMATRIX system (Philips, Andover, MA, USA) was used, which was equipped with a highly ergonomic X5-1 transducer for RT3DE acquisition. Transthoracic 3D images (Figure 6) were taken from the apical window during a deep breath-hold with the patient in the lateral decubitus position. Full-volume 3D volumetric data were obtained by combining four ECG-triggered, wedge-shaped sub-volumes. The recorded RT3DE data sets included the complete MV anatomic apparatus, and the entire LV in the pyramidal data set. Frame rates (16-22 frames/s) were selected based on imaging depth (12-16 cm). The 3D images were digitally stored by experienced sonographers and then transferred to a work station. I used commercially available Q-lab 3D computer software (Philips, Andover, MA, USA) to determine the LV end-diastolic and end-systolic volumes (LVEDV and LVESV) (Figure 7) [42]. The cavity of the LV in each image plane was manually traced, and the LV volume was calculated using the multiplanar Simpson method. Ejection fraction (EF %) was calculated by: EF% = 100 x (LVEDV - LVESV)/LVEDV [37].

The echocardiography was performed by echocardiographers and cardiologists (with clinical internships less than four years). The measurement accuracy was periodically

checked by intra-devices variability (the same subject was measured by all devices, then the variability of the results checked.) and by inter- and intra-observer variability (mostly carried out between the echocardiographers), according to the guidelines of the Japanese Society of Echocardiography [41].

Figure 6. Full-volume 3D volumetric data using 3D echocardiography.

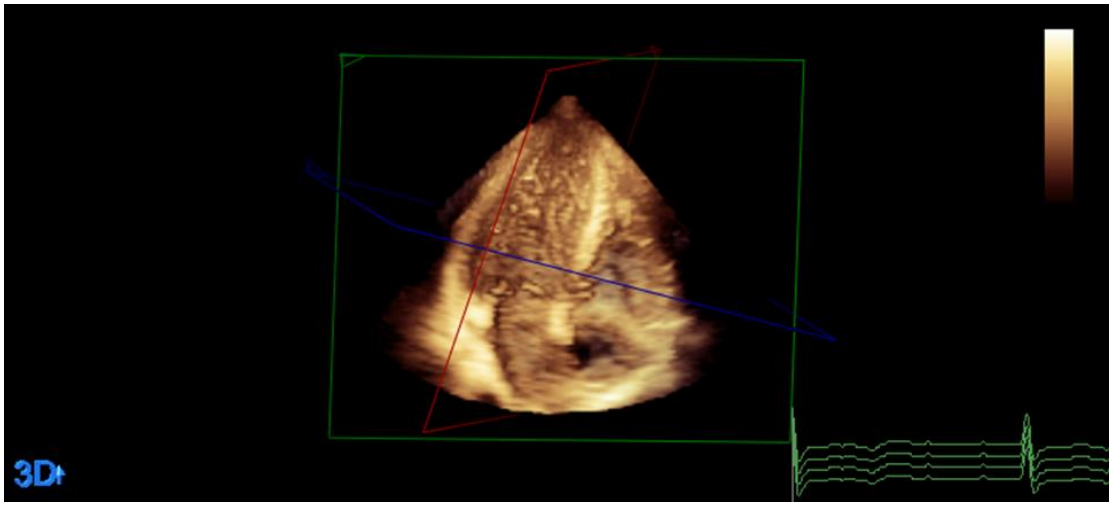

Full-volume 3D volumetric data including the whole heart were obtained in the apical window using RT3DE.
RT3DE, real-time 3D echocardiography.

Figure 7. Measurements of left ventricular end-diastolic volume using Q-lab 3D computer software.

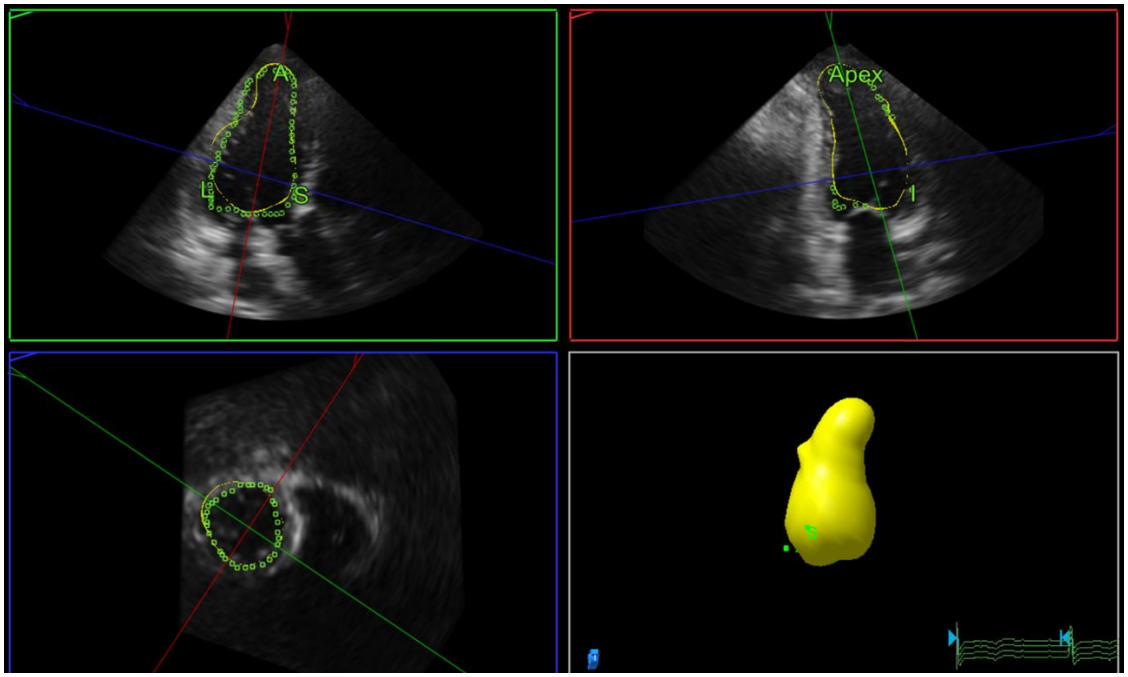

The cavity of the LV in each image plane was manually traced, and the LV volume was calculated using the multiplanar Simpson method.
LV, left ventricle.

4. 3D echocardiographic quantification of the mitral complex

Custom software (Realview^{TM}, YD, NARA, Japan) was used to analyze the mitral complex geometry from the RT3DE volume data, as described previously [28, 43, 44]. Initially, the time of MV closure onset was identified. The 3D volumetric image was automatically cropped into 18 sequential planes spaced at equal radial distances (10°). Then the anterior-posterior (A-P) and medial-lateral (M-L) plane of the MV annulus position was objectively determined by the aortic valvular and MV geometries among these planes. Subsequently, the sagittal planes of the MV depicted in all 18 sequential plane images were traced. From the above, 3D images of the mitral complex were finally reconstructed automatically. Additionally, the timing of mid-systole was determined and the 3D reconstruction of the mitral apparatus repeated in the same manner as described above (Figure 8).

From these reconstructed 3D images of the MV apparatus, MV parameters were calculated by Realview at the time of MV closure and mid-systole, as previously described [28, 43, 44]. These parameters included the MV annular area, annular circumferences, annular diameter (A-P and M-L), annular height (from the saddle-shaped mitral annulus by a non-planar index), mean and maximum tenting length, tenting volume, and tenting area (Figure 8). The saddle-shaped mitral annulus was

located in a plane, while the distance between the leaflets and the mitral annulus was maintained. The maximum tenting length was calculated as the distance from the annular plane to the most distant tethering site of the leaflet, and the mean tenting length was calculated as the average distance between the annular plane and the tethered leaflets. Tenting volume was determined as the volume enclosed between the annular plane and the mitral leaflets. MV leaflet size was determined as the tenting area at the time of MV closure onset. MV coaptation-zone area was calculated by subtracting the MV tenting area at mid-systole from the MV tenting area at the MV closure onset (Figure 8).

Figure 8. The quantity of mitral complex by real-time 3D echocardiography.

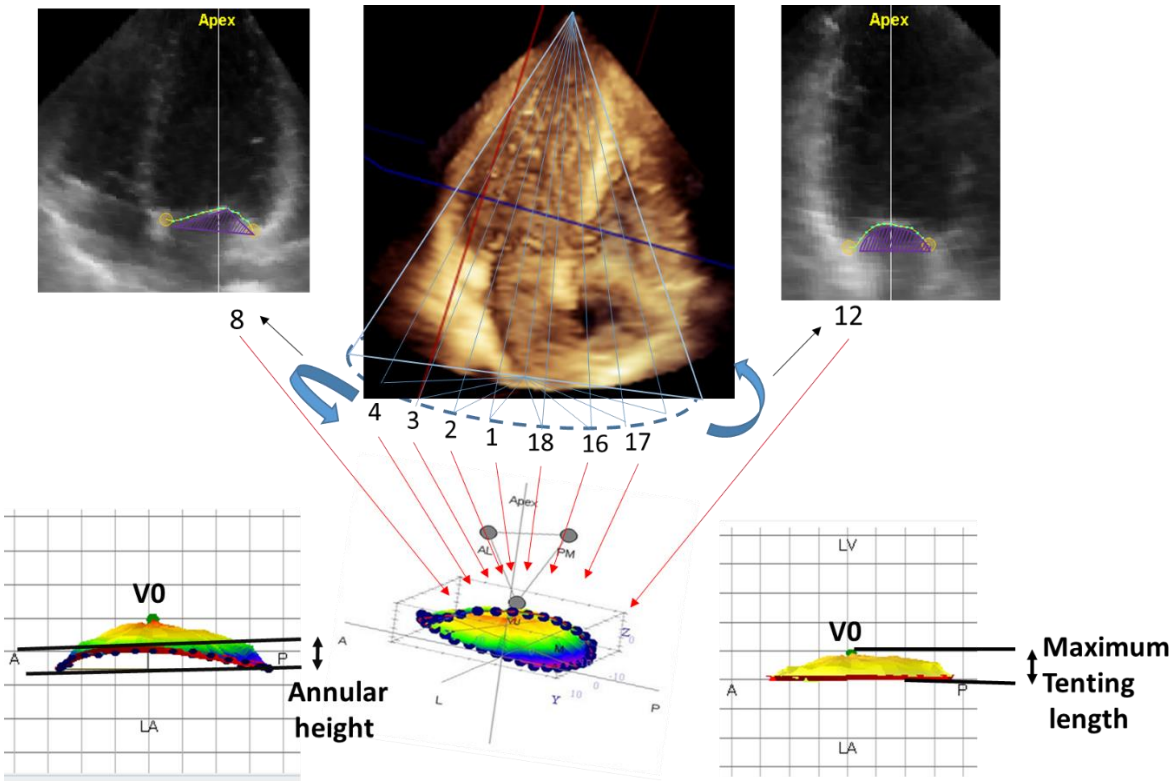

Sagittal images (8, 12) of the MV at the time of MV closure onset among 18 equally-segmented rotated images, which were automatically obtained from the 3D volumetric image. The yellow points represent the mitral annulus in the sagittal plane. The green points represent the MV leaflets in the frontal plane. The mitral annulus and the traced mitral leaflets were marked in the same way on each of the 18 equally-segmented rotated images.

Then, 3D images of the mitral annulus and leaflets were automatically constructed by rotation of the MV annulus in the sagittal plane and MV leaflets in the frontal plane in each segmented image, and these images were used to quantify the parameters of MV geometry at the onset of MV closure. The same images of the mitral apparatus at mid-systole were also completed.

AL and **PM**, antero-lateral and postero-medial papillary muscle. **Maximum tenting length** is the distance between Vo and annular plane. **Mean tenting length** is the average distance between the annular plane and the leaflets. The purple area (images 8, 12) in each of 18 segmented images rotated automatically forming the **tenting volume**. **MV**, mitral valve. **V0**, the endpoint of the maximum tenting length in coaptation.

5. Reproducibility of 3D echo quantification of mitral leaflets

For assessing the reproducibility of 3D echo quantification of mitral leaflet size and coaptation-zone areas, two independent observers were invited to perform 3D echocardiographic measurements. Each observer repeated the measurements subsequently in 10 cases respectively, and in the different cardiac cycles.

6. Statistical analysis

All data were expressed as the mean ± SD for continuous variables and as percentages for categorical variables, and all statistical analyses were conducted utilizing SPSS24.0 software (SPSS Inc, Chicago, IL, USA). Intra-observer and inter-observer variability, inter-beat variability of the MV leaflet area, and MV base-clear zone area were assessed by intra-class correlation coefficient analysis. Pearson's linear correlation analysis was used to determine correlations between the MV parameters and the echocardiographic and clinical variables. Multivariable linear regression was performed to assess the factors that determined the MV leaflet area and coaptation-zone area. Variables with $p<0.10$ in univariable analysis were incorporated into the multivariable linear regression model. Statistical significance was defined as a two-tailed p-value < 0.05.

Results

Intra-observer and inter-observer variabilities of MV leaflet measurements using 3D software showed good reproducibility and are summarized in Table 1. Out of 386 enrolled cases, 211 were considered to be inadequate for 3D echo analysis on account of poor 3D echocardiographic images of MV. By the time of the accepted publication of the first part of this step 1 study [45], there were 135 analyzed cases in the manuscript. As cases were continuously enrolled until 31 December 2017, 3D echo analysis was ultimately performed in 175 out of 386 cases (45.3 %) in this step of the study (Figure 9). Although patients with FMR were not excluded, none of the patients had significant (more than mild) FMR (trivial MR, 150 cases (85.7%); mild MR, 7 cases (4.0%)) (Figure 9). Table 2 shows the characteristics of 175 patients and the results of 3D measurements of the LV and conventional echocardiographic parameters. The results of 3D measurements of MV parameters are summarized in Table 3. The average MV leaflet area was 10.7±1.7 cm^2, and the average MV coaptation-zone area was 1.8±0.7 cm^2. A significant relationship between MV leaflet area and coaptation-zone area was first found ($r=0.481$, $p<0.001$) (Figure 10A). Then, a significant relationship between MV leaflet area/BSA and coaptation-zone area/BSA was found ($r=0.590$, $p<0.001$) (Figure 10B).

Table 1. Intra-observer and inter-observer variability and intra-beat and inter-beat variability of MV leaflet area and basal-clear zone area

Intra-class correlation coefficients				
	Intra-observer	P-value	Inter-observer	P-value
MV leaflet area	0.934	<0.001	0.826	<0.001
MV base-clear zone area	0.954	<0.001	0.874	<0.001
			Inter-beat	P-value
MV leaflet area			0.747	<0.001
MV base-clear zone area			0.708	<0.001

MV, mitral valvular.

Figure 9. The study cases in study 1.

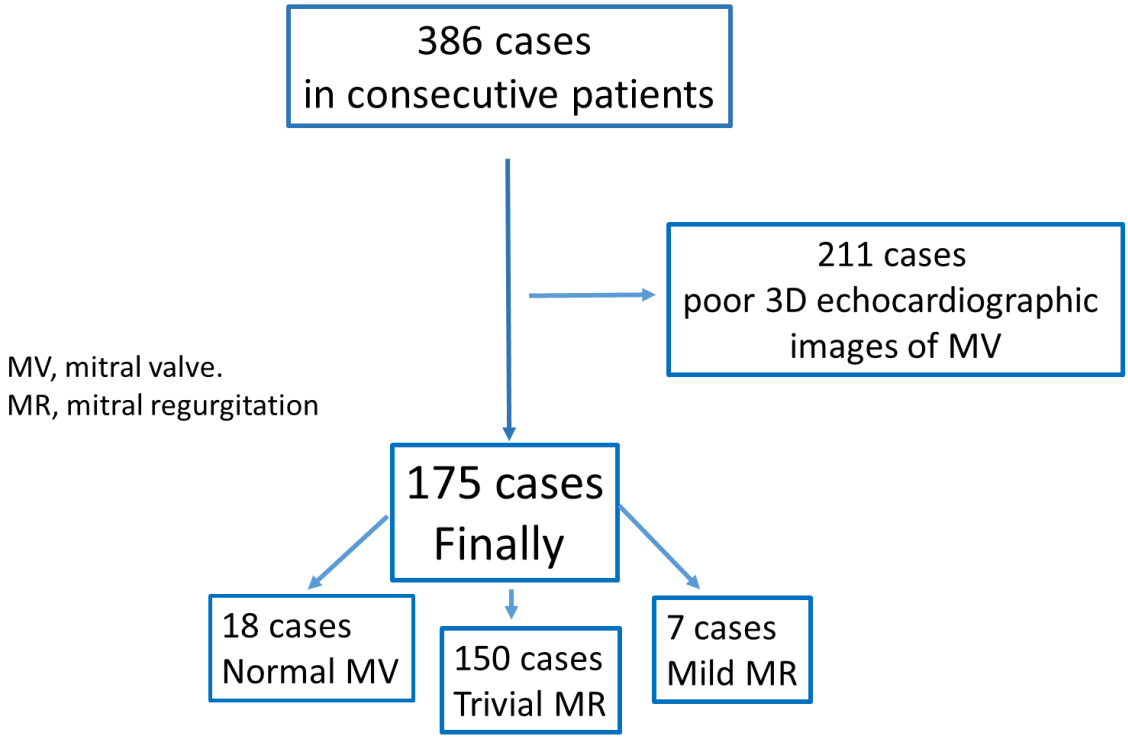

Finally there were 175 cases were enrolled in study 1.

Table 2. Patient characteristics and echocardiography (Step 1 of the study)

Variables	n =175
Age (years)	61 ± 15
Male	87 (49.7 %)
Body surface area (m^2)	1.7 ± 0.2
Body mass index (kg/m^2)	24.0 ± 4.2
Heart rate (bpm)	70 ± 12
Systolic blood pressure (mmHg)	137 ± 22
Diastolic blood pressure (mmHg)	76 ± 13
Comorbidities	
Hypertension	79 (45.1%)
Type II diabetes mellitus	21 (12.0%)
Dyslipidemia	60 (34.3%)
Coronary artery disease	13 (7.4%)
Ischemic stroke	5 (2.9%)
Chronic kidney disease	31 (17.7%)
Hemodialysis	5 (2.9%)
Smoking	23 (13.1%)
3D Echocardiography	
LVEDV index (ml/m^2)	56.5 ± 8.1
LVESV index (ml/m^2)	20.0 ± 4.6
LV ejection fraction (%)	64.8 ± 5.5
2D echocardiography	
LV mass index (g/m^2)	78.7 ± 15.8
LA volume index (ml/m^2)	28.7± 9.2
E/A	1.0 ± 0.4
Septal e’	6.4 ± 2.5
E/e’	11.9 ± 4.2

LVEDV and LVESV, left ventricular end-diastolic and end-systolic volumes; LV, left ventricular; LA, left atrial.

Table 3. Mitral valve geometric parameters at the onset of MV closure and mid-systole

MV variables	At MV closure onset		At mid-systole	
	Mean ± SD	Range	Mean ± SD	Range
Annular area (cm^2)	8.4 ± 1.2	5.6 ~ 11.5	7.3 ±1.1	4.6 ~ 10.3
Annular circumference (mm)	103.5 ± 7.2	84.2 ~ 121.1	96.7 ±7.5	76.7 ~ 114.5
AP – diameter (mm)	31.7 ±2.3	25.8 ~ 38.1	29.6 ±2.4	23.3 ~ 35.8
ML – diameter (mm)	33.4 ±2.5	26.6 ~ 39.3	30.9 ±2.5	23.5 ~ 36.4
Annular height (mm)	3.1 ±0.6	0.9 ~ 4.9	3.9 ±0.7	1.5 ~ 5.6
Max tenting length (mm)	6.5 ±1.9	3.0 ~ 14.2	4.9 ±1.9	1.6 ~ 11.4
Mean tenting length (mm)	3.2 ±1.2	0.8 ~ 7.9	1.9 ±1.2	-0.1 ~ 5.6
Tenting volume (cm^3)	2.1 ±0.9	0.6 ~ 5.2	1.2 ±0.6	0.2 ~ 3.3
Leaflet area (cm^2)	10.7 ±1.7	7.0 ~ 15.3	—	—
Base-clear zone area (cm^2)	—	—	8.9 ±1.5	5.1 ~ 14.2
Coaptation-zone area (cm^2)	—	—	1.8±0.7	0.2 ~ 4.0

AP, anterior-posterior; MV, mitral valve; ML, medial-lateral.

Figure 10. (A) Correlation between the mitral valvular leaflet area and coaptation-zone area. (B) Correlation between the mitral valvular leaflet area/BSA and coaptation-zone area/BSA

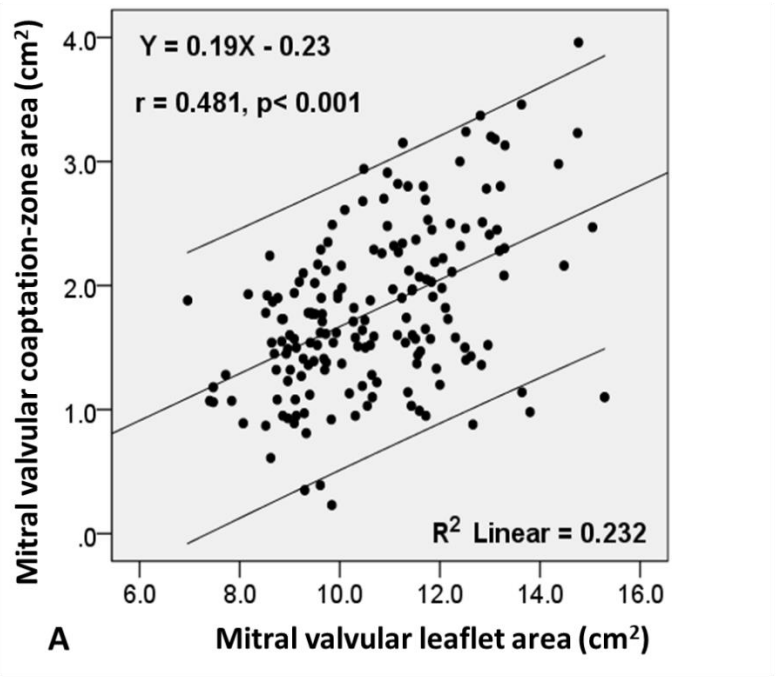

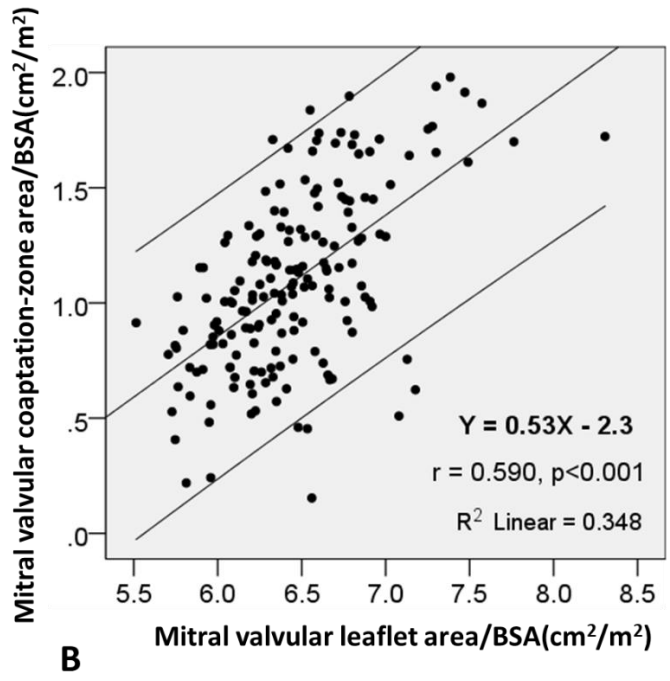

(A) MV leaflet area was significantly associated with MV coaptation-zone area.
(B) MV leaflet area/BSA was significantly associated with MV coaptation-zone area/BSA

BSA, Body surface area.

In the general healthy population, echocardiographic parameters may change according to body size, age, or heart size. Thus, I selected BSA, BMI, age, and LV size, but not other clinical factors, and examined which parameters were adequate to index mitral leaflet area in patients with normal LV size and function. Then, among body size, age, and LV size, the association between MV leaflet area and BSA were compared in order to identify the major determinants of the MV leaflet area. Therefore, body mass index (BMI), age, and LV volume were obtained by RT3DE, to explore which was the major determinant of MV leaflet area among body size, age, and LV size in subjects without LV dilatation. From that, the MV leaflet area was found to be strongly and positively associated with BSA ($r=0.907$, $p<0.001$). It also had a significant but weaker association with age, LVEDV, and LVESV (Figure 11, Table 4). In multivariable analysis, BSA and LVEDV were the parameters independently and positively associated with the MV leaflet area (Table 4). When the same univariable analyses were repeated for the MV coaptation-zone area, there were significant associations with BSA, age, LVEDV, and LVESV (Figure 12, Table 5), but these were weaker than those with the MV leaflet area. In multivariable analysis, LVEDV was independently and positively associated with the MV coaptation-zone area (Table 5). When the independent associations of the clinical factors were compared with the MV leaflet area and coaptation-zone area, BSA had a

greater influence on the MV leaflet area, whereas LVEDV had a greater influence on the MV coaptation-zone area.

Figure 11. Correlations between mitral valvular leaflet area and body surface area (A), age (B), left ventricular end-diastolic volume (C), and left ventricular end-systolic volume (D).

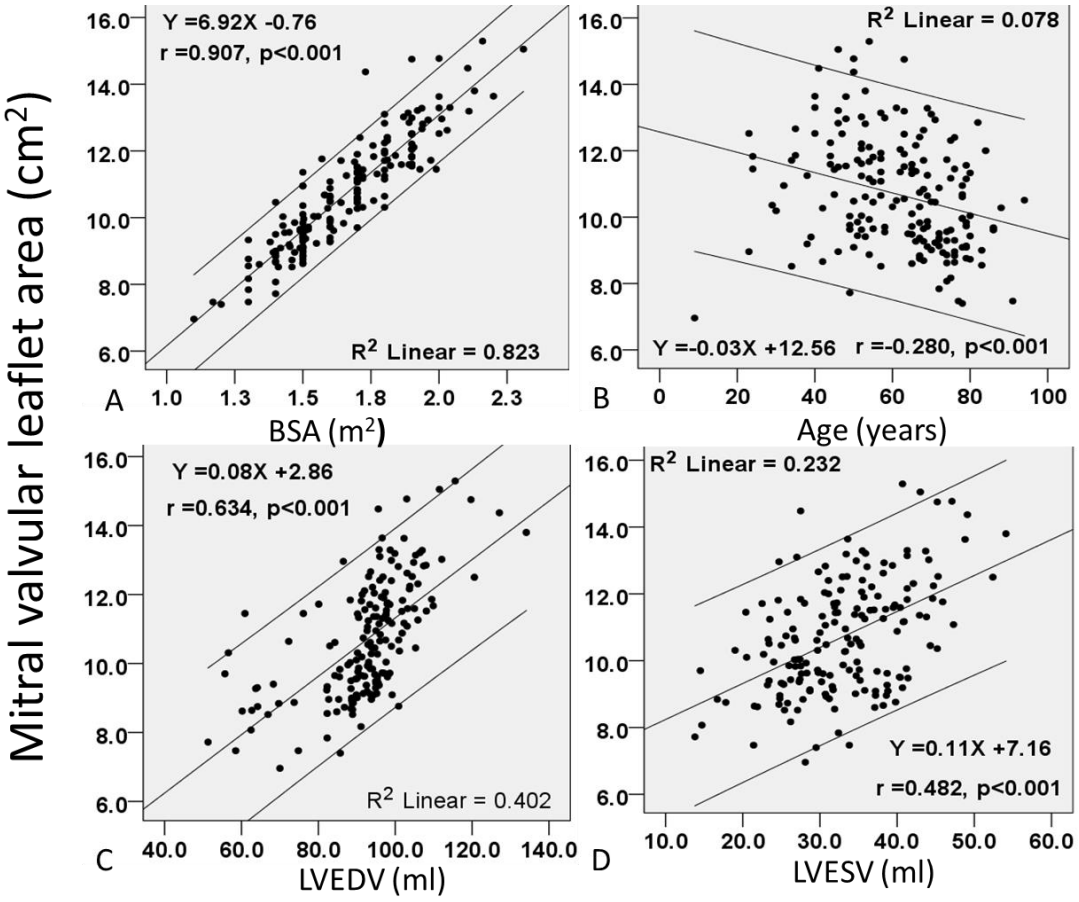

MV leaflet area was more strongly associated with BSA than with age, LVESV, or LVEDV.

Table 4. Univariable and multivariable analyses of the relationships of MV leaflet area with BSA, BMI, and age, and LV volume

Variables	MV leaflet area (cm^2)	
Univariable analysis		
	Correlation coefficient	P-value
BSA (m^2)	0.907	<0.001
BMI (kg/m^2)	0.649	<0.001
Age (years)	-0.280	<0.001
LVEDV (ml)	0.634	<0.001
LVESV (ml)	0.482	<0.001
Multivariable analysis		
	Standardized coefficient	P-value
BSA (m^2)	0.736	<0.001
BMI (kg/m^2)	0.058	0.088
Age (years)	-0.018	0.489
LVEDV (ml)	0.276	<0.001
LVESV (ml)	0.028	0.471

BSA, body surface area; BMI, body mass index; LVEDV and LVESV, left ventricular end-diastolic and end-systolic volumes; MV, mitral valvular.

Table 5. Univariable and multivariable analyses of the relationships of MV coaptation-zone area with BSA, BMI, age, and LV volume

Variables	MV coaptation-zone area (cm^2)	
Univariate analysis		
	Correlation coefficient	P-value
BSA (m^2)	0.257	0.001
BMI (kg/m^2)	0.140	0.064
Age (years)	-0.208	0.006
LVEDV (ml)	0.434	<0.001
LVESV (ml)	0.380	<0.001
Multivariable analysis		
	Standardized coefficient	P-value
BSA (m^2)	0.088	0.390
BMI (kg/m^2)	-0.048	0.610
Age (years)	-0.119	0.106
LVEDV (ml)	0.324	0.004
LVESV (ml)	0.092	0.389

BSA, body surface area; BMI, body mass index; LVEDV and LVESV, left ventricular end-diastolic and end-systolic volumes; MV, mitral valvular.

Figure 12. Correlations between mitral valvular coaptation-zone area and body surface area (A), age (B), left ventricular end-diastolic volume (C), and left ventricular end-systolic volume (D).

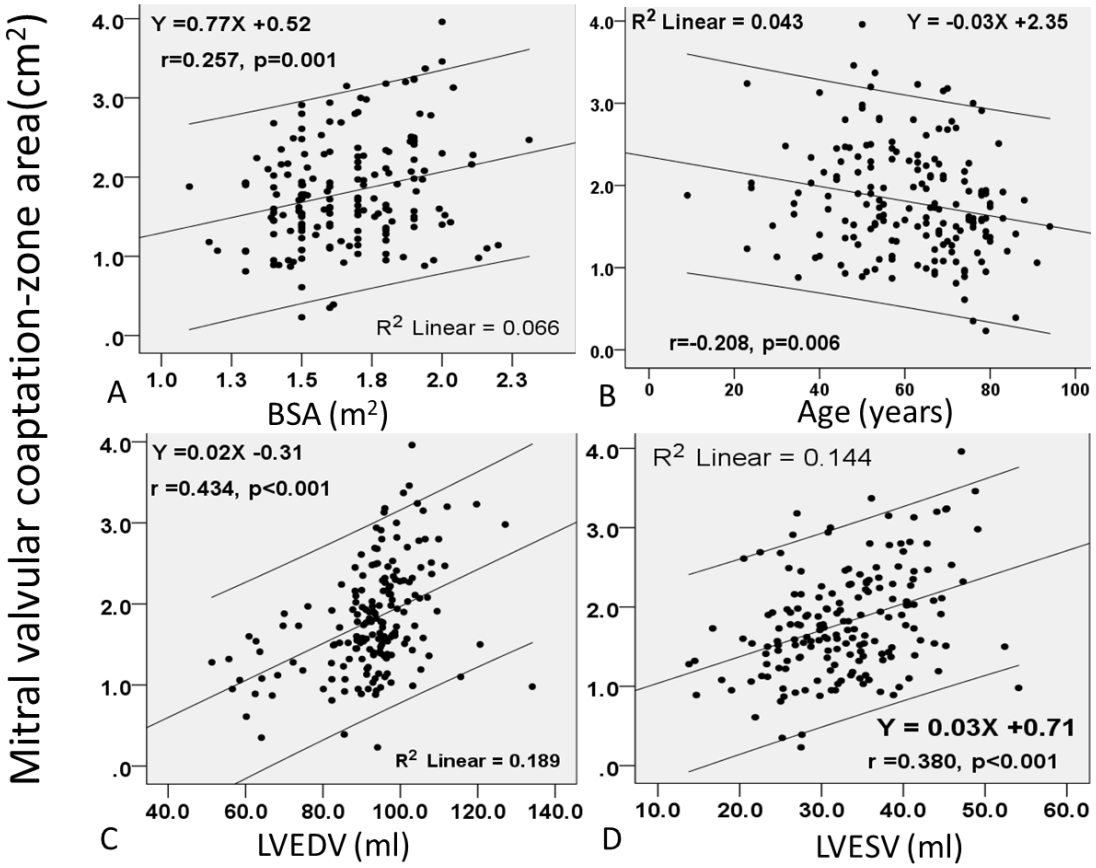

MV coaptation-zone area was significantly but weakly associated with BSA, age, LVESV, and LVEDV.

BSA, body surface area; LVEDV/SV, left ventricular end-diastolic volume/ end-systolic volume; MV, mitral valve.

In light of the close relationship between MV leaflet area and BSA, MV leaflet area and coaptation-zone area were indexed by BSA. In addition, MV coaptation-zone area was also indexed by MV leaflet area. The associations between these indexed parameters and the clinical and echocardiographic parameters were examined by univariable and multivariable linear regression analyses (Table 6, 7, 8). In univariable analysis, MV leaflet area/BSA was significantly associated with diastolic blood pressure, a history of hemodialysis, LVEDV index, and LVESV index (Table 6); MV coaptation-zone area/BSA was significantly associated with the presence of CAD, LVEDV index, and LVESV index (Table 7); MV coaptation-zone area/MV leaflet area was significantly associated with the presence of CAD, LVEDV index, and LVESV index (Table 8). In multivariable analysis, diastolic blood pressure and LVEDV index were independently associated with MV leaflet area/BSA (Table 6); the LVEDV index was independently associated with MV coaptation-zone area/BSA (Table 7); Presence of CAD and LVEDV index were independently associated with MV coaptation-zone area/BSA (Table 8).

Table 6. Univariable and multivariable analyses of MV leaflet area/BSA with clinical factors

Variables	MV leaflet area /BSA (cm^2/m^2)	
	Correlation coefficient	P-value
Univariable analysis		
Age (years)	-0.089	0.240
Male	0.121	0.110
Heart rate (bpm)	-0.067	0.383
Systolic BP (mmHg)	0.050	0.514
Diastolic BP (mmHg)	0.195	**0.010**
Hypertension	-0.006	0.939
Type II diabetes mellitus	-0.025	0.741
Dyslipidemia	0.078	0.306
Coronary artery disease	0.007	0.922
Ischemic stroke	-0.029	0.699
Chronic kidney disease	0.051	0.502
Hemodialysis	0.226	**0.003**
Smoking	-0.045	0.556
LVEDV index (ml/m^2)	0.469	**<0.001**
LVESV index (ml/m^2)	0.423	**<0.001**
LA volume index (ml/m^2)	0.045	0.553
Multivariable analysis		
	Standardized coefficient	P-value
Diastolic BP (mmHg)	0.262	**<0.001**
Hemodialysis	0.078	0.238
LVEDV index (ml/m^2)	0.370	**<0.001**
LVESV index (ml/m^2)	0.168	0.082

BSA, body surface area; BP, blood pressure; LVEDV and LVESV, left ventricular end-diastolic and end-systolic volumes; LA, left atrial; MV, mitral valve.

Table 7. Univariable and multivariable analyses of MV coaptation-zone area/BSA with the clinical factors

Variables	MV coaptation-zone area/BSA (cm^2/m^2)	
	Correlation coefficient	P-value
Univariable analysis		
Age (years)	-0.127	0.095
Male	-0.028	0.710
Heart rate (bpm)	-0.067	0.381
Systolic BP (mmHg)	-0.019	0.805
Diastolic BP (mmHg)	0.070	0.359
Hypertension	-0.061	0.424
Type II diabetes mellitus	-0.059	0.436
Dyslipidemia	0.053	0.485
Coronary artery disease	-0.162	**0.032**
Ischemic stroke	-0.081	0.288
Chronic kidney disease	0.003	0.966
Hemodialysis	0.091	0.230
Smoking	-0.024	0.748
LVEDV index (ml/m^2)	0.386	**<0.001**
LVESV index (ml/m^2)	0.336	**<0.001**
LA volume index (ml/m^2)	-0.025	0.746
Multivariable analysis		
	Standardized coefficient	P-value
Age (years)	-0.136	0.060
Coronary artery disease	-0.132	0.062
LVEDV index (ml/m^2)	0.340	**0.001**
LVESV index (ml/m^2)	0.082	0.424

BSA, body surface area; BP, blood pressure; LVEDV and LVESV, left ventricular end-diastolic and end-systolic volumes; LA, left atrial; MV, mitral valve.

Table 8. Univariable and multivariable analyses of MV coaptation-zone area/ MV leaflet area with the clinical factors

Variables	MV coaptation-zone area/MV leaflet area (cm^2/cm^2)	
	Correlation coefficient	P-value
Univariable analysis		
Age (years)	-0.129	0.089
Male	-0.059	0.434
Heart rate (bmp)	-0.059	0.436
Systolic BP (mmHg)	-0.035	0.650
Diastolic BP (mmHg)	0.030	0.694
Hypertension	-0.067	0.375
Type II diabetes mellitus	-0.068	0.370
Dyslipidemia	0.038	0.617
Coronary artery disease	-0.182	**0.016**
Ischemic stroke	-0.089	0.244
Chronic kidney disease	-0.009	0.909
Hemodialysis	0.043	0.570
Smoking	-0.019	0.799
LVEDV index (ml/m^2)	0.343	**<0.001**
LVESV index (ml/m^2)	0.291	**<0.001**
LA volume index (ml/m^2)	-0.038	0.614
Multivariable analysis		
	Standardized coefficient	P-value
Age (years)	-0.132	0.072
Coronary artery disease	-0.153	**0.034**
LVEDV index (ml/m^2)	0.316	**0.003**
LVESV index (ml/m^2)	0.056	0.596

BSA, body surface area; BP, blood pressure; LVEDV and LVESV, left ventricular end-diastolic and end-systolic volumes; LA, left atrial; MV, mitral valve.

Step 2 study

Aims

Based on the results of the first step, I aimed to determine if the MV coaptation-zone area was associated with the severity of atherosclerosis as assessed by cardio-ankle vascular index (CAVI) or by other clinical factors in patients with normal LV systolic function and size, by RT3DE.

Methods

1. Study subjects

For the second step of the study, 3D echocardiographic volume data were also determined in consecutive subjects who underwent conventional echocardiography using iE33 (Philips, Andover, MA, USA) for screening or assessing cardiac diseases, from 8 October 2015 to 31 December 2019. These subjects visited our hospital for medical care, a health check, or a preliminary investigation of disease. Out of the pooled 3D data sets, subjects were consecutively examined with 2D echocardiographic screening and CAVI screening criteria and then added to the retrospective 3D echocardiographic analysis.

2D echocardiographic screening criteria were examined in subjects with normal LV dimensions (an indexed LV end-diastolic diameter; males < 3.2cm/m^2, females < 3.3

cm/m^2) [46] and systolic function (LV ejection fraction ≥ 50%) [47], without regional or global LV wall motion abnormalities in a variety of clinical conditions. Next, patients were excluded who suffered from cardiomyopathy, atrial fibrillation, or significant valvular heart disease, except FMR, for the reason that these diseases per se could influence the mitral leaflet size [19, 23, 27, 28]. Furthermore, according to a previous study that reported normal values of 3D echocardiographic measurements and their gender differences, the step 2 study finally enrolled only cases who appeared to have normal LV size by 3D echocardiographic measurements (LV end-diastolic volume index of 26~74 ml/m^2 for males, and 28~64 ml/m^2 for females) [38]. The clinical data were recorded on each patient at the time of the first diagnosis and during the follow-up period from the case history. By looking at the patient's history, it was determined if they had hypertension, diabetes, dyslipidemia, CAD, CKD, ischemic stroke, or a regular smoking habit, and if they had been on hemodialysis. Patients with peripheral artery disease (stenosis or occlusion of the abdominal aorta, iliac artery, and/or lower extremity arteries) [48] were excluded, because CAVI does not serve as a surrogate of arterial stiffness in patients with these diseases. This cross-sectional study was approved by the institutional ethics committee of the University of Tokyo (# 2650), and the requirement of informed consent was waived because only de-identified data routinely

collected during daily practice were used. This step of the study enrolled 112 patients.

2. Conventional echocardiography

Conventional echocardiography was performed consecutively in the same manner as in the step 1 study.

3. 3D echocardiographic data acquisition and LV volume, CAVI measurements

The iE33xMATRIX system (Philips, Andover, MA, USA) specially devised with a highly ergonomic X5-1 transducer for RT3DE acquisition was used for taking 3D echocardiography. Transthoracic 3D images were acquired from the apical window during a deep breath-holding period in the same manner as in the step 1 study.

Cardio-ankle vascular index was measured by the VS2000 system (Fukuda, Tokyo, Japan), and the mean CAVI was calculated as an average value of the right and left CAVI.

All the above echocardiographic and CAVI measurements were checked and taken by echocardiographers and cardiologists. The date of CAVI measurements mostly was before the echocardiographic examinations with mean 652±822 days (range -273 ~ 3341 days). The accuracy was periodically checked by intra-device variability (the same

subject was measured by all devices, then the variability of the results examined) and by inter- and intra-observer variability (mainly carried out between the echocardiographers), in accordance with the guidelines of the Japanese Society of Echocardiography [41].

4. 3D echocardiographic quantification of the mitral complex

Custom software (Realview, YD, NARA, Japan) was used for analyzing the mitral complex geometry from the RT3DE volume data, following the same method as used previously [28, 43, 44]. MV leaflets and coaptation-zone areas were determined in the same manner as in the step 1 study.

5. Statistical analysis

All data were presented as the mean ± SD for continuous variables and as percentages for categorical variables, and all statistical analyses were calculated using SPSS24.0 software (SPSS Inc, Chicago, IL, USA). Pearson's linear correlation was used to determine the associations between the MV parameters and echocardiographic and clinical variables. Multivariable linear regression analysis was applied to assess the factors that determined the MV leaflet area and coaptation-zone area. Variables with $p<0.10$ in univariate analysis were selected and included in a multivariable linear regression model. Statistical significance was determined as a two-tailed p-value < 0.05.

Results

Out of the 112 cases enrolled, 46 were considered to be inadequate for 3D echo analysis because of poor 3D echocardiographic images of the MV. Consequently, 3D echo analysis and CAVI were performed in 66 out of 112 cases (58.9%) in the step 2 study (Figure 13). Although patients with FMR were not excluded, none of the patients had significant MR in step 2. Trivial MR was seen in 55 cases (83.3%) and mild MR in 4 cases (6.1%) out of the 66 subjects (Figure 13).

Table 9 shows the characteristics of 66 patients and the results of 3D measurements of the LV and conventional echocardiographic parameters. The results of 3D measurements of MV parameters are summarized in Table 10. The average MV leaflet area was 10.7±1.4 cm^2, and the average MV coaptation-zone area was 1.3±0.4cm^2.

Figure 13. The study cases in study 2.

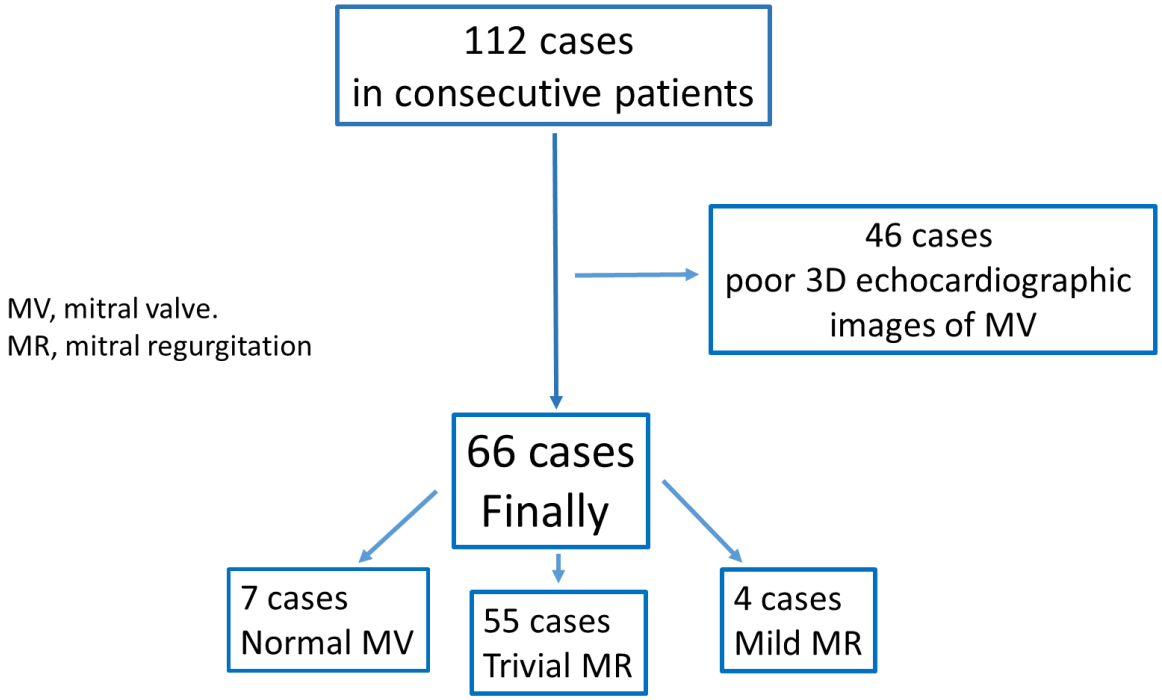

Finally, there were 66 cases were enrolled in study 2.

Table 9. Patient characteristics, echocardiography and CAVI (step 2 study)

Variables	n =66
Age (years)	66 ± 13
Male	42 (63.6 %)
Body surface area (m^2)	1.7 ± 0.2
Body mass index (kg/m^2)	24.3 ± 4.4
Heart rate (bpm)	69 ± 11
Systolic blood pressure (mmHg)	136 ± 23
Diastolic blood pressure (mmHg)	73 ± 14
Comorbidities	
Hypertension	41 (62.1%)
Type II diabetes mellitus	26 (39.4%)
Dyslipidemia	33 (50%)
Coronary artery disease	21 (31.8%)
Ischemic stroke	6 (9.1%)
Chronic kidney disease	16 (24.2%)
Hemodialysis	2 (3%)
Smoking	16 (24.2%)
3D Echocardiography	
LVEDV index (ml/m^2)	54.5 ± 6.1
LVESV index (ml/m^2)	20.3 ± 3.0
LV ejection fraction (%)	62.8 ± 3.4
2D echocardiography	
LV mass index (g/m^2)	84.7 ± 20.2
LA volume index (ml/m^2)	31.9 ± 10.7
E/e’	12.9 ± 4.3
Right CAVI	8.6 ±1.5
Left CAVI	8.6 ±1.6
Mean CAVI	8.6 ±1.5

LVEDV and LVESV, left ventricular end-diastolic and end-systolic volumes; LV, left ventricular; LA, left atrial; CAVI, cardio-ankle vascular index.

Table 10. Mitral valve geometrical parameters at the onset of MV closure and cardiac mid-systole

MV variables	At MV closure onset		At cardiac mid-systole	
	Mean ± SD	Range	Mean ± SD	Range
Annular area (cm^2)	8.6 ± 1.0	6.7 ~ 11.5	7.7 ±1.0	5.6 ~ 10.3
Annular circumference (mm)	104.7 ± 6.3	92.0~ 121.1	99.4 ±6.3	84.6 ~ 114.5
Leaflet area (cm^2)	10.7 ±1.4	8.35 ~ 15.1	—	—
Basal-clear-zone area (cm^2)	—	—	9.4 ±1.2	7.0 ~ 12.6
Coaptation-zone area (cm^2)	—	—	1.3±0.4	0.8~ 2.5

MV, mitral valve.

According to the step1 study, MV leaflet and coaptation-zone areas were indexed by BSA. In addition, MV coaptation-zone area was also indexed by MV leaflet area. The associations between these indexed parameters and the clinical and echocardiographic parameters were examined by univariable and multivariable linear regression analyses (Table 11, 12, 13). In the univariable analyses of MV leaflet area/BSA and clinical factors, age and mean CAVI was significantly associated with MV leaflet area/BSA ($r = -0.464$, $p<0.001$, table 11, Figure 14A). In the multivariable analysis, mean CAVI was the only factor independently associated with MV leaflet area/BSA ($r = -0.440$, $p=0.015$, table 11). In the univariable analysis of table 12, MV coaptation-zone area/BSA was significantly associated with age, hypertension, dyslipidemia, echocardiographic LV diastolic parameter E/e', and mean CAVI. Among them, MV coaptation-zone area/BSA was strongly associated with mean CAVI ($r= -0.740$, $p<0.001$, Figure 14B). In the multivariable analysis shown in table 12, mean CAVI was independently associated with MV coaptation-zone area/BSA ($r = -0.611$, $p<0.001$). In the univariable analysis of table 13, MV coaptation-zone area/MV leaflet area was significantly associated with age, hypertension, echocardiographic LV diastolic parameter E/e', and mean CAVI. Among them, MV coaptation-zone area/ MV leaflet area was strongly associated with mean CAVI ($r= -0.695$, $p<0.001$, Figure 15). In the

multivariable analysis shown in table 13, mean CAVI was independently associated with MV coaptation-zone area/MV leaflet area ($r = -0.530$, $p < 0.001$).

Table 11. Univariable and multivariable analyses of MV leaflet area/BSA with clinical factors

Variables	MV leaflet area/BSA (cm^2/m^2)	
Univariable analysis		
	Correlation coefficient	P-value
Age (years)	-0.335	**0.006**
Heart rate (bpm)	0.058	0.646
Systolic BP (mmHg)	-0.171	0.169
Diastolic BP (mmHg)	-0.067	0.592
Hypertension	-0.069	0.583
Type II diabetes mellitus	-0.127	0.309
Dyslipidemia	-0.189	0.129
Coronary artery disease	0.052	0.676
Ischemic stroke	0.096	0.442
Chronic kidney disease	0.134	0.282
Hemodialysis	0.002	0.987
Smoking	0.132	0.291
LVEDV index (ml/m^2)	-0.026	0.837
LVESV index (ml/m^2)	0.130	0.296
LV ejection fraction (%)	-0.237	0.055
LV mass index (g/ m^2)	-0.037	0.768
LA volume index (ml/m^2)	0.022	0.861
E/e’	-0.107	0.391
Mean CAVI	-0.464	**<0.001**
Multivariable analysis		
	Standardized coefficient	P-value
Age (years)	0.010	0.955
LV ejection fraction (%)	-0.143	0.217
Mean CAVI	-0.440	**0.015**

BSA, body surface area; BP, blood pressure; LV, left ventricle; LVEDV and LVESV, left ventricular end-diastolic and end-systolic volumes; LA, left atrial; MV, mitral valve; CAVI, cardio-ankle vascular index.

Table 12. Univariable and multivariable analyses of MV coaptation-zone area/BSA with the clinical factors

Variables	MV coaptation-zone area/BSA (cm^2/m^2)	
Univariable analysis		
	Correlation coefficient	P-value
Age (years)	-0.626	**<0.001**
Heart rate (bpm)	-0.129	0.307
Systolic BP (mmHg)	-0.204	0.100
Diastolic BP (mmHg)	0.109	0.384
Hypertension	-0.272	**0.027**
Type II diabetes mellitus	-0.204	0.100
Dyslipidemia	-0.247	**0.045**
Coronary artery disease	-0.215	0.083
Ischemic stroke	-0.104	0.405
Chronic kidney disease	-0.085	0.499
Hemodialysis	-0.040	0.747
Smoking	-0.037	0.769
LVEDV index (ml/m^2)	0.040	0.748
LVESV index (ml/m^2)	0.126	0.312
LV ejection fraction (%)	-0.145	0.246
LV mass index (g/m^2)	-0.146	0.242
LA volume index (ml/m^2)	-0.072	0.567
E/e’	-0.445	**<0.001**
Mean CAVI	-0.740	**<0.001**
Multivariable analysis		
	Standardized coefficient	P-value
Age (years)	-0.102	0.454
Hypertension	0.073	0.493
Dyslipidemia	-0.085	0.435
Coronary artery disease	-0.064	0.482
E/e’	-0.113	0.298
Mean CAVI	-0.611	**<0.001**

BSA, body surface area; BP, blood pressure; LV, left ventricle; LVEDV and LVESV, left ventricular end-diastolic and end-systolic volumes; LA, left atrial; MV, mitral valve; CAVI, cardio-ankle vascular index.

Table 13. Univariable and multivariable analyses of MV coaptation-zone area/MV leaflet area with the clinical factors

Variables	MV coaptation-zone area/MV leaflet area (cm^2/cm^2)	
Univariable analysis		
	Correlation coefficient	P-value
Age (years)	-0.598	**<0.001**
Heart rate (bmp)	-0.149	0.235
Systolic BP (mmHg)	-0.190	0.127
Diastolic BP (mmHg)	0.126	0.312
Hypertension	-0.280	**0.023**
Type II diabetes mellitus	-0.197	0.113
Dyslipidemia	-0.231	0.062
Coronary artery disease	-0.242	0.051
Ischemic stroke	-0.129	0.304
Chronic kidney disease	-0.121	0.334
Hemodialysis	-0.042	0.739
Smoking	-0.063	0.613
LVEDV index (ml/m^2)	0.053	0.671
LVESV index (ml/m^2)	0.114	0.364
LV ejection fraction (%)	-0.109	0.385
LV mass index (g/m^2)	-0.151	0.226
LA volume index (ml/m^2)	-0.080	0.525
E/e’	-0.456	**<0.001**
Mean CAVI	-0.695	**<0.001**
Multivariable analysis		
	Standardized coefficient	P-value
Age (years)	-0.112	0.440
Hypertension	0.048	0.669
Dyslipidemia	-0.031	0.792
Coronary artery disease	-0.105	0.277
E/e’	-0.164	0.158
Mean CAVI	-0.530	**<0.001**

BSA, body surface area; BP, blood pressure; LV, left ventricle; LVEDV and LVESV, left ventricular end-diastolic and end-systolic volumes; LA, left atrial; MV, mitral valve; CAVI, cardio-ankle vascular index.

Figure 14. Correlations between mitral valvular leaflet area/ BSA, coaptation-zone area/BSA, and mean CAVI.

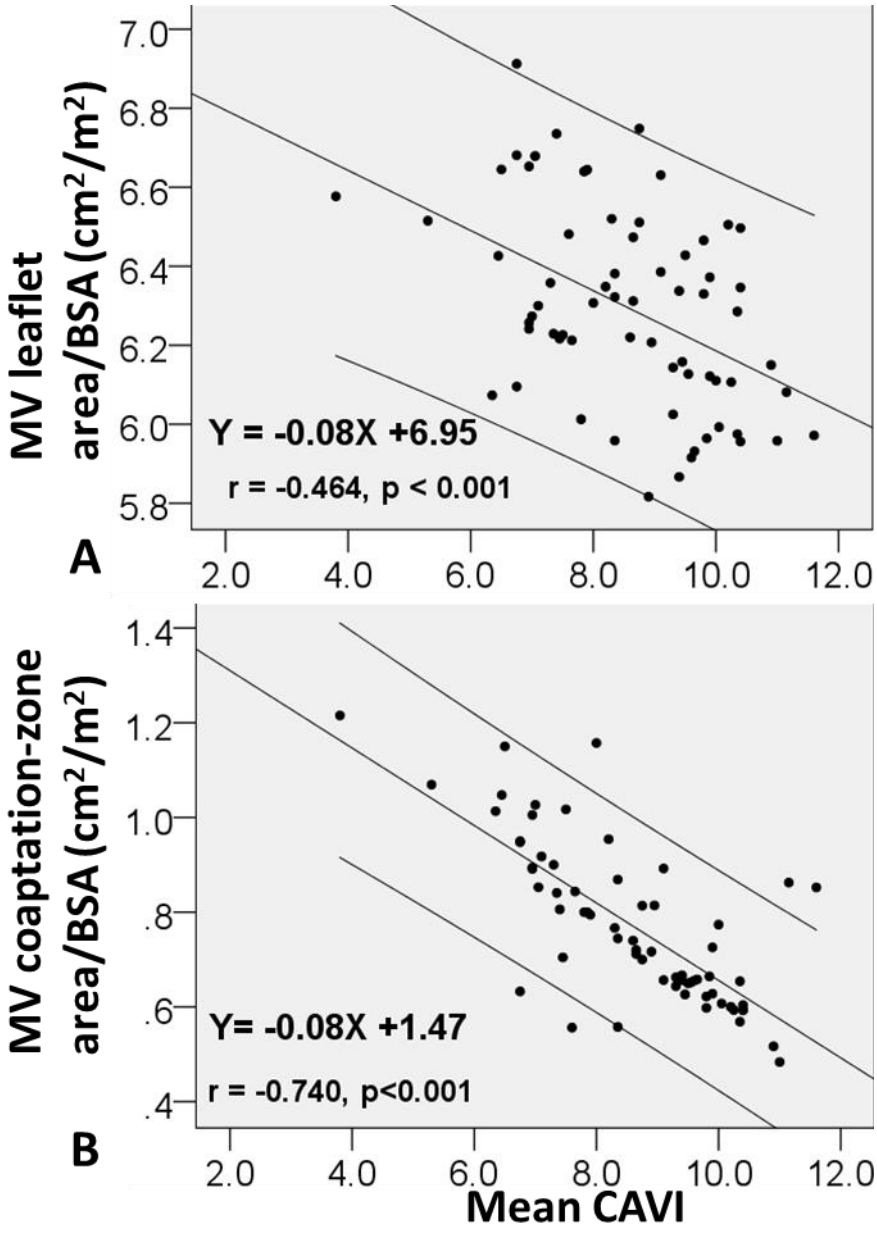

A. MV leaflet area/ BSA was associated with mean CAVI.

B. MV coaptation-zone area/BSA was associated with mean CAVI.

BSA, body surface area; CAVI, cardio-ankle vascular index; MV, mitral valve

Figure 15. Correlations between MV coaptation-zone area /MV leaflet area and mean CAVI.

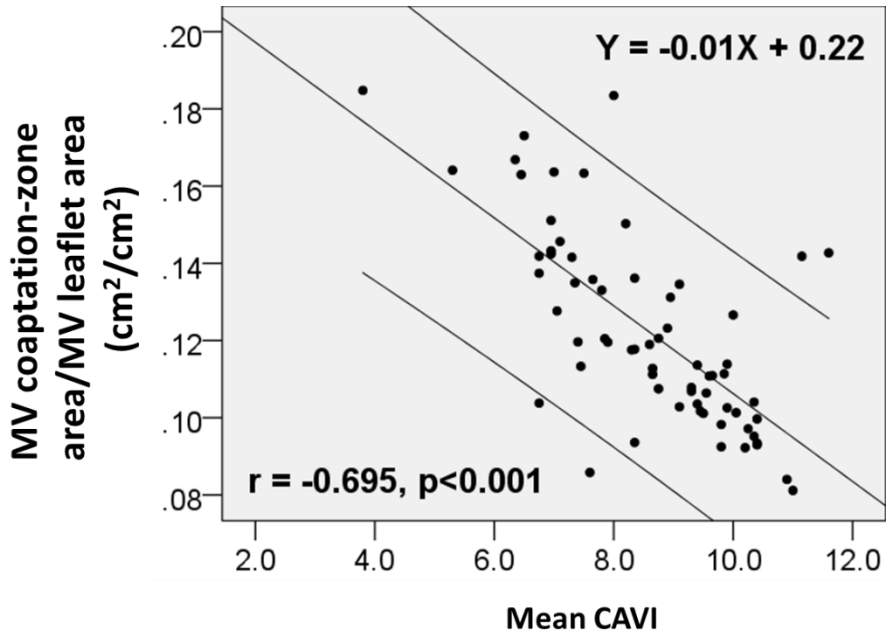

MV coaptation-zone area/MV leaflet area was associated with mean CAVI.

CAVI, cardio-ankle vascular index; MV, mitral valve

Discussion

In the first step study, only 175 (45%) cases out of 386 enrolled cases were eligible for 3D analysis, because precise 3D measurements of the mitral complex required acquisition of clear entire 3D volume data of the mitral complex consisting of 18 equally-segmented images. Then a significant relationship between MV leaflet area and coaptation-zone area was found in subjects who appeared to have a preserved LV ejection fraction without LV dilation. In addition, MV leaflet area and coaptation-zone area were linearly correlated with BSA. When the clinical factors associated with MV leaflet size and coaptation-zone size were explored, the major findings were as follows:

(1.1) Body size was the strongest determinant of the MV leaflet area. The size of the mitral leaflet area might be intrinsically determined by body size in subjects with normal LV size and EF.

(1.2) MV leaflet area/BSA was relatively constant, regardless of differences in clinical factors when LV size was normal. However, the LVEDV index or other clinical factors, such as diastolic blood pressure, may be associated with MV leaflet area/BSA. In particular, the LVEDV index was an important determinant of the MV leaflet area.

(1. 3) MV coaptation-zone area was also associated with BSA. However, it showed more dispersion and variability compared with the MV leaflet area associated with BSA, and

its index with BSA was determined mainly by the LVEDV index rather than other clinical factors in the presence of normal LV size. MV coaptation-zone area index with MV leaflet area was also determined mainly by the LVEDV index, As compared with MV coaptation-zone area/BSA, CAD was independently and negatively associated with MV coaptation-zone area/MV leaflet area.

MV leaflet varied widely among individual patient

Previous investigations have demonstrated that the measurement of MV annular, tenting, and papillary muscle parameters varied widely among individual patients [43]. Ultrastructural and cellular changes in the mitral leaflets due to chronic mechanical loading have been reported [49]. Also, reductions of cell number and disoriented collagen fibers increased elastin fibers, and decreased mucopolysaccharides were observed histologically in the MV of individuals over 60 years of age [50]. Furthermore, other studies have indicated that the MV leaflets are active living structures with their own metabolic and compensatory mechanisms and that their structure can be modified by various clinical factors [35, 36, 51–53]. However, unlike the aortic valve, structural changes in the MV leaflets related to age, atherosclerosis, and other clinical factors are not well understood.

The determinants of MV leaflet area in normal LV size

As shown in the step 1 study, the MV leaflet area had a significant relationship with the MV coaptation-zone area, indicating the importance of MV leaflet size for proper MV closure in patients with normal LV size. A reduced MV leaflet area even in patients with normal LV size could result in a reduced MV coaptation-zone area and the generation of FMR. Furthermore, the MV leaflet area was associated with BSA, age, and LV size in univariable analysis, and the strongest association was with BSA. Although the MV leaflet area decreased slightly with age, age was not independently associated with MV leaflet area in multivariable analysis. Therefore, decreased MV area with aging might be mainly related to decreased body size during aging. It is known that LV size can be increased in patients with acquired conditions that require high cardiac output, such as athletes [54], those with anemia, and those on hemodialysis [55]. However, the step 1 study suggests that the most important intrinsic determinant of mitral leaflet size might be body size. The results suggest that it might be reasonable to index the MV leaflet area by BSA for comparison among individuals with different clinical characteristics.

The determinants of MV coaptation–zone area in normal LV size

MV coaptation-zone area was also associated with BSA. But this association was weaker than the association of the MV leaflet area with BSA. Besides, LVEDV was the

only independent determinant of the MV coaptation-zone area, suggesting there is a close relationship between MV coaptation-zone area and LV size. As previous studies suggested [19, 23, 27, 28], the MV coaptation-zone area, which is an essential component of complete MV closure, is significantly influenced by tethering and the subvalvular apparatus, and the determinants of MV coaptation-zone area might be more diverse and complicated than the determinants of MV leaflet area size. This might account for the result of larger dispersion and variability in the MV coaptation-zone area than the dispersion in MV leaflet size in the present step of this study.

The influence of clinical factors on the MV leaflet area/BSA

To examine the influence of clinical factors on the MV leaflet area when BSA was accounted for, the factors associated with MV leaflet area/BSA were explored. Lower diastolic blood pressure was independently associated with a decreased MV leaflet area /BSA and a larger LVEDV index and also was independently related to a larger MV leaflet area /BSA. In particular, LVEDV was strongly associated with MV leaflet area/BSA. Since LV size can be changed in response to acquired conditions or various heart diseases, the MV leaflet area might be stretched according to LV size. From that, LV remodeling enlargement is the most important factor among the acquired clinical factors, even in patients without significant LV dilation. On the other hand, the

associations between MV leaflet area/BSA and the clinical factors other than LV size were weak or not significant. Consequently, MV leaflet size could be influenced by these clinical factors, but it was mainly determined by body size, and MV leaflet area/BSA should remain relatively constant as long as LV size remains within normal limits.

Lower diastolic blood pressure is recognized as a surrogate for increased arterial stiffness [56]. In this study, patients did not appear to have any significant aortic regurgitation. From that, lower diastolic blood pressure was presumably associated with advanced atherosclerosis [57, 58]. Degenerative changes due to atherosclerosis, represented by decreased diastolic blood pressure, might be associated with degenerative changes in MV tissue and decreased MV leaflet area and might be attenuated the compensatory mechanism. In patients with advanced atherosclerosis, a reduced MV leaflet area might be one of the mechanisms for FMR.

The influence of clinical factors on MV coaptation-zone area/BSA and MV coaptation-zone area/MV leaflet area

In the present results, MV coaptation-zone area/BSA was significantly reduced in patients with CAD. Reduced MV coaptation-zone in CAD may be a risk factor for FMR

in ischemic patients with relatively mild LV dilation compared with patients with idiopathic dilated cardiomyopathy. One possible explanation for decreased MV coaptation in CAD is a degenerative change in the MV coaptation-zone in association with systemic atherosclerosis. Reduced MV leaflet size and coaptation–zone area in patients with CAD due to atherosclerosis might be associated with a high prevalence of FMR. Although patients with LV regional wall motion abnormalities were excluded by the visual assessment on echocardiography, latent contractile abnormalities caused by CAD might lead to a decreased coaptation-zone area. However, only 13 patients with apparent CAD were included in this study. Further investigation with a larger number of CAD patients is needed to address this issue. MV coaptation-zone area/MV leaflet area was also determinate by LVEDV index as MV coaptation-zone area and MV leaflet area were. However, pathological determinants including CAD might be different among these parameters and remains to be explored in further studies.

In the second step of the study, the associations of atherosclerosis and other clinical factors with MV leaflets and coaptation-zone areas indexed with BSA were explored. The major findings were as follows:

(2.1) the reductions of MV leaflet and coaptation-zone area/BSA and MV coaptation-

zone area/MV leaflet area were independently and positively associated with mean CAVI, the stronger of those relations being with MV coaptation-zone area/BSA.

(2.2) MV leaflet area/BSA was relatively constant, regardless of differences in the clinical factors other than mean CAVI (including age and LV ejection fraction) when LV remained normal in size and function. The major finding of the observation about MV coaptation-zone area/BSA and MV coaptation-zone area/MV leaflet area were as follows.

(2.3) MV coaptation-zone area was relatively constant, regardless of differences in the clinical factors other than mean CAVI (including age, hypertension, dyslipidemia, coronary artery disease, and echocardiographic LV diastolic parameter E/e'). However, mean CAVI was the only clinical factor that was independently associated with MV coaptation-zone area/BSA. MV coaptation-zone area/MV leaflet area was similarly relatively constant, regardless of associating with age, hypertension, echocardiographic LV diastolic parameter E/e'.

Relationship between MV leaflets and atherosclerosis

CAVI is widely used for assessing atherosclerosis as a blood pressure-independent parameter of arterial stiffness at measuring time and reported to be associated with

cardiovascular risks and events [59,60]. The results of step 2 suggested that reductions of both the MV leaflet and coaptation-zone area were independently associated with the mean CAVI when BSA was accounted for. This suggests that atherosclerosis, which was represented by mean CAVI, might be associated with degenerative changes in the MV leaflet tissue and decreased MV coaptation-zone area.

In histology, the cross-sectional structure of MV leaflets is divided into three layers (atrialis, spongiosa, fibrosa). In the atrialis layer, there are endothelium, subendothelial connective tissue, and elastin sheets, which have the same histological structure as in vascular layers, for maintaining the elasticity of the leaflets [61]. Pathological studies [62] have indicated that foam cells appear in early atherosclerotic lesions [63], and can also be found in affected patients on the endothelium of mitral leaflets.

Consequently, in patients with advanced atherosclerosis, the atrialis layer of MV leaflets might be degenerated, presenting with a reduction of the MV leaflet area and coaptation ability, which might be one of the mechanisms for the pathology of FMR.

Relationship between MV leaflets and clinical factors other than mean CAVI

The MV leaflet area/BSA was relatively constant, regardless of differences in the

clinical factors other than mean CAVI, which included age and LV ejection fraction when LV was kept within normal size and function. Ultrastructural and cellular changes in the mitral leaflets due to chronic mechanical loading have been reported [49]. It is because of this that mechanical loading from the SBP, LVESV index or LV ejection fraction might reduce the MV leaflet area/BSA if the LV has any pathological processes. In our observations, the MV leaflet area/BSA was relatively constant because of the presence of normal LV function. A reduction in cellularity, disoriented collagen fibers, and increased elastin fibers with reduced mucopolysaccharides has been seen in the mitral valves of individuals over 60 years of age [50]. Consequently, the structure of MV leaflets, which are active living structures with their own metabolic and compensatory mechanisms, can be modified by various clinical factors [35, 36, 51–53] when LV loses its normal size.

Observation on MV coaptation-zone area/BSA and MV coaptation-zone area/ MV leaflet area, and other clinical factors other than mean CAVI;

The MV coaptation-zone area was relatively constant, regardless of differences in the clinical factors other than mean CAVI, which included age, hypertension, dyslipidemia, coronary artery disease, and echocardiographic LV diastolic parameter E/e'), in the presence of normal LV size and function. It is because of this that the microcirculation

in the MV annulus and leaflet transition zone [64–67] gives insufficient support to the MV leaflet intrinsic metabolism, reducing the MV coaptation size in hypertension and coronary artery disease. However, only 26 patients with type II diabetes mellitus were included in this step of the study. Further investigation with a larger number of patients with coronary artery disease is needed to address this issue. Dyslipidemia increases blood viscosity together with hypertension, causing increased shear stress on the MV coaptation-zone. Consequently, MV coaptation can be attenuated. Owing to the same pathology as the MV leaflet, the MV coaptation-zone is also affected by the aging process when cardiac aging occurs. When compare between MV coaptation-zone area/BSA and MV coaptation-zone area/MV leaflet area, they are both relatively constant, but the results indicated that MV coaptation-zone area/MV leaflet area was less sensitive to systemic pathological factor such as dyslipidemia.

Consequently, the MV coaptation was relatively constant under conditions of normal LV function and was independently associated only with the mean CAVI.

Limitations

For both steps of the study, the MV area was calculated at the onset of mitral leaflet

closure. However, it has been shown that the mitral leaflet stretches during systole [68]. Accordingly, the mitral leaflet area measurements and also the coaptation-zone area may have been underestimated. However, this should not affect the associations between the coaptation-zone area and the clinical factors. Since this study was conducted in a single-center, there may have been some selection bias in the study population. It is also noteworthy that in this study, MV geometry was evaluated by 3D echocardiography. Although the advances made in 3D echocardiography have been remarkable, it still has limited spatial and temporal resolutions. Further advancement of 3D echocardiography or other imaging modalities may bring greater and more precise insight into this research area. Finally, the study subjects did not include patients with significant FMR. It is because I consecutively enrolled patients with normal LV size and function. As a result, none of enrolled patients had significant MR unfortunately. Therefore, further study is needed to examine the relationship between the MV leaflet area and the mechanisms of FMR. Nevertheless, the study is the first to provide some insight into the clinical factors that can reduce the MV leaflet coaptation-zone area, which might increase the risk of progressively poor clinical FMR.

Conclusions

Even in patients with normal LV systolic function and size, MV leaflet size had a significant impact on competent MV coaptation. MV leaflet area might be intrinsically determined more by body size than age and LV size, while the MV leaflet area/BSA is relatively constant. LVEDV might be associated with a reduction of the MV leaflet area. MV coaptation-zone area might be reduced during the progression of atherosclerosis. LV diastolic function was the determinant of the MV coaptation-zone area. Coronary artery disease might reduce the MV coaptation-zone area.

Acknowledgments

I thank Prof. Yutaka Yatomi and Dr. Masao Daimon for their helpful and inspirational guidance and advice on the conduct and design of the study, as well as with the interpretation of the findings. This study would not have been possible without their input, time, and experience.

I would also like to thank Prof. Issei Komuro, Dr. Hiroyuki Morita, Dr. Takayuki Kawata, Dr. Tomoko Nakao, Dr. Koki Nakanishi, Dr. Megumi Hirokawa, Dr. Naoko Sawada, Dr. Koichi Kimura, Dr. Yuko Yamanaka, in the Department of Clinical Laboratory and Department of Cardiovascular Medicine for their helpful technical advice regarding the methodology, design, and interpretation of the results of this study.

References

[1] Rossi A, Dini FL, Faggiano P, Agricola E, Cicoira M, Frattini S, Simioniuca., Gullace M, Ghio S, Enriquez-Sarano M, Temporelli PL. Independent prognostic value of functional mitral regurgitation in patients with heart failure. A quantitative analysis of 1256 patients with ischaemic and non-ischaemic dilated cardiomyopathy. Heart;97:1675–80 (2011).

[2] Kaneko H, Suzuki S, Uejima T, Kano H, Matsuno S, Takai H, Oikawa Y, Yajima J, Aizawa T, Yamashita T. Functional mitral regurgitation and left ventricular systolic dysfunction in the recent era of cardiovascular clinical practice, an observational cohort study. Hypertens Res;37:1082–7 (2014).

[3] Shah T, Zhong M, Minutello RM. Functional mitral regurgitation in heart failure. Cardiol Rev;27:327–36 (2019).

[4] Yiu SF, Enriquez-Sarano M, Tribouilloy C, Seward JB, Tajik AJ. Determinants of the degree of functional mitral regurgitation in patients with systolic left ventriculardDysfunction. Circulation;102:1400–6 (2000).

[5] Asgar AW, Mack MJ, Stone GW. Secondary mitral regurgitation in heart failure: Pathophysiology, prognosis, and therapeutic considerations. J Am Coll Cardiol;65:1231–48 (2015).

[6] Lancellotti P, Zamorano J-L, Vannan MA. Imaging Challenges in Secondary Mitral Regurgitation. Circ Cardiovasc Imaging;7:735–46 (2014).

[7] Lebrun F, Lancellotti P, Piérard LA. Quantitation of functional mitral regurgitation during bicycle exercise in patients with heart failure. J Am Coll Cardiol;38:1685–92 (2001).

[8] Lancellotti P, Gérard PL, Piérard LA. Long-term outcome of patients with heart failure and dynamic functional mitral regurgitation. Eur Heart J;26:1528–32 (2005).

[9] Gertz ZM, Raina A, Saghy L, Zado ES, Callans DJ, Marchlinski FE, Keane MG, Silvestry FE. Evidence of atrial functional mitral regurgitation due to atrial fibrillation: Reversal with arrhythmia control. J Am Coll Cardiol;58:1474–81 (2011).

[10] Takahashi Y, Abe Y, Sasaki Y, Bito Y, Morisaki A, Nishimura S, Shibata T. Mitral valve repair for atrial functional mitral regurgitation in patients with chronic atrial fibrillation. Interact Cardiovasc Thorac Surg;21:163–8 (2015).

[11] Abe Y, Akamatsu K, Ito K, Matsumura Y, Shimeno K, Naruko T, Takahashi Y, Shibata T, Yoshiyama M. Prevalence and prognostic significance of functionalitral and tricuspid regurgitation despite preserved left ventricular

ejection fraction in atrial fibrillation Patients. Circ J;82:1451–8 (2018).

[12] Ito K, Abe Y, Takahashi Y, Shimada Y, Fukumoto H, Matsumura Y, Naruko T, Shibata T, Yoshiyama M, Yoshikawa J. Mechanism of atrial functional mitral regurgitation in patients with atrial fibrillation: A study using three-dimensional transesophageal echocardiography. J Cardiol;70:584–90 (2017).

[13] Delgado V, Bax JJ. Atrial functional mitral regurgitation: from mitral annulus dilatation to insufficient leaflet remodeling. Circ Cardiovasc Imaging;10:1–3 (2017).

[14] Van der Bijl P, Vo NM, Leung M, Ajmone Marsan N, Delgado V, Stone GW, Bax JJ. Impact of atrial fibrillation on improvement of functional mitral regurgitation in cardiac resynchronization therapy. Hear Rhythm;15:1816–22 (2018).

[15] Liang JJ, Silvestry FE. Mechanistic insights into mitral regurgitation due to atrial fibrillation: “Atrial functional mitral regurgitation.” Trends Cardiovasc Med;26:681–9 (2016).

[16] Silbiger JJ. Mechanistic insights into atrial functional mitral regurgitation: Far more complicated than just left atrial remodeling. Echocardiography;36:164–9 (2019).

[17] Bursi F, Enriquez-Sarano M, Nkomo VT, Jacobsen SJ, Weston SA, Meverden RA, Roger VL. Heart failure and death after myocardial infarction in the community: the emerging role of mitral regurgitation. Circulation;111:295–301 (2005).

[18] Lamas GA, Mitchell GF, Flaker GC, Smith SC, Gersh BJ, Basta L, Moye L, Braunwald E, Pfeffer MA. Clinical Significance of mitral regurgitation after acute myocardial infarction. Circulation;96:827–33 (1997).

[19] Chaput M, Handschumacher MD, Tournoux F, Hua L, Guerrero JL, Vlahakes GJ, Levine RA. Mitral leaflet adaptation to ventricular remodeling occurrence and adequacy in patients with functional mitral regurgitation. Circulation;118:845–52 (2008).

[20] Varma PK, Krishna N, Jose RL, Madkaiker AN. Ischemic mitral regurgitation. Ann Card Anaesth;20:432–9 (2017).

[21] De Marchena E, Badiye A, Robalino G, Junttila J, Atapattu S, Nakamura M, Canniere DD, Salerno T. Respective prevalence of the different carpentier classes of mitral regurgitation: a stepping stone for future therapeutic research and development. J Card Surg;26:385–92 (2011).

[22] Poglajen G, Harlander M, Gersak B. Ex vivo study of altered mitral apparatus

geometry in functional mitral regurgitation. Heart Surg Forum;13:E172-6 (2010).

[23] Debonnaire P, Al Amri I, Leong DP, Joyce E, Katsanos S, Kamperidis V, Schalij JM, Bax JJ, Marsan AN, Delgado V. Leaflet remodelling in functional mitral valve regurgitation: Characteristics, determinants, and relation to regurgitation severity. Eur Heart J Cardiovasc Imaging;16:290–9 (2015).

[24] Lancellotti P, Moura L, Pierard LA, Agricola E, Popescu BA, Tribouilloy C, Hagendorff A, Monin J-L, Badano L, Zamorano JL. European Association of Echocardiography recommendations for the assessment of valvular regurgitation. Part 2: mitral and tricuspid regurgitation (native valve disease). Eur J Echocardiogr;11:307–32 (2010).

[25] Daimon M, Saracino G, Fukuda S, Koyama Y, Kwan J, Song JM, Kongsaerepong V, Agler DA, Thomas JD, Shiota T. Dynamic change of mitral annular geometry and motion in ischemic mitral regurgitation assessed by a computerized 3D echo method. Echocardiography;27:1069–77 (2010).

[26] Daimon M, Saracino G, Gillinov AM, Koyama Y, Fukuda S,Kwan J, Song JM, Kongsaerepong V, Agler AD, Thomas DJ, Shiota T. Local dysfunction and asymmetrical deformation of mitral annular geometry in ischemic mitral regurgitation: A novel computerized 3D echocardiographic analysis.

Echocardiography;25:414–23 (2008).

[27] Beaudoin J, Handschumacher MD, Zeng X, Hung J, Morris EL, Levine RA, Schwammenthal E. Mitral valve enlargement in chronic aortic regurgitation as a compensatory mechanism to prevent functional mitral regurgitation in the dilated left ventricle. J Am Coll Cardiol;61:1809–16 (2013).

[28] Saito K, Okura H, Watanabe N, Obase K, Tamada T, Koyama T, Hayashida A, Neishi Y, Kawamoto T, Yoshida K. Influence of chronic tethering of the mitral valve on mitral leaflet size and coaptation in functional mitral regurgitation. JACC Cardiovasc Imaging;5:337–45 (2012).

[29] Judge DP, Markwald RR, Hagège AA, Levine RA. Translational research on the mitral valve: from developmental mechanisms to new therapies. J Cardiovasc Transl Res;4:699–701 (2011).

[30] Alghamdi AA., Elmistekawy EM, Singh SK, Latter D A. Is concomitant surgery for moderate functional Mitral regurgitation indicated during aortic valve replacement for aortic stenosis? a systematic review and evidence-based recommendations. J Card Surg;25:182–7 (2010).

[31] Waisbren EC, Stevens LM, Avery EG, Picard MH, Vlahakes GJ, Agnihotri AK. Changes in Mitral regurgitation after replacement of the stenotic aortic valve.

Ann Thorac Surg;86:56–62 (2008).

[32] Caballero-Borrego J, Gómez-Doblas JJ, Cabrera-Bueno F, García-Pinilla JM, Melero JM, Melero JM, Porras C, Olalla E, Teresa Galvan E De. Incidence, associated factors and evolution of non-severe functional mitral regurgitation in patients with severe aortic stenosis undergoing aortic valve replacement. Eur J Cardio-Thoracic Surg;34:62–6 (2008).

[33] Rossi A, Dandale R, Nistri S, Faggiano P, Cicoira M, Benfari G, Onorati F, Santini F, Messika-Zeitoun D, Enriquez-Sarano M, Vassanelli C. Functional mitral regurgitation in patients with aortic stenosis: prevalence, clinical correlates and pathophysiological determinants: a quantitative prospective study. Eur Heart J Cardiovasc Imaging;15:631–6 (2014).

[34] Cohoon KP, Criqui MH, Budoff MJ, Lima JA, Blaha MJ, Decker PA, Durazo R, Liu K, Kramer H. Relationship of aortic wall distensibility to mitral and aortic valve calcification: The Multi-Ethnic Study of Atherosclerosis. Angiology;69:443–8 (2018).

[35] Dal-Bianco JP, Aikawa E, Bischoff J, Guerrero JL, Handschumacher MD, Sullivan S, Johnson B, Titus JS, Iwamoto Y, Wylie-sears J, Levine RA, Carpentier A. Active adaptation of the tethered mitral valve.

Circulation;120:334–42 (2009).

[36] Marsit O, Clavel MA, Côté-Laroche C, Hadjadj S, Bouchard MA, Handschumacher MD, Clisson M, Drolet MC, Boulanger M, Kim D, Guerrero JL, Bartko PE, Couet J, Arsenault M, Mathieu P, Pibarot P, Aikawa M, Mathieu P. Pibarot P, Aikawa E, Bischoff J, Levine RA, Beaudoin J. Attenuated mitral leaflet enlargement contributes to functional mitral regurgitation after myocardial infarction. J Am Coll Cardiol;75:395–405 (2020).

[37] Lang RM, Badano LP, Mor-Avi V, Afilalo J, Armstrong A, Ernande L, Flachskampf FA, Foster E, Goldstein SA, Kuznetsova T, Lancellotti P, Muraru D, Picard MN, Rietzschel ER, Rudski L, Spencer KT, Tsang W, Voigt J-U. Recommendations for cardiac chamber quantification by echocardiography in adults: an update from the American Society of Echocardiography and the European Association of Cardiovascular Imaging. Eur Hear J – Cardiovasc Imaging;16:233–71 (2015).

[38] Fukuda S, Watanabe H, Daimon M, Abe Y, Hirashiki A, Hirata K, Ito H, Iwai-Takano M, Iwakura K, Izumi C, Hidaka T, Yuasa T, Murata K, Nakatani S, Negishi K, Nishigami K, Nishikage T, Ota T, Hayashida A, Sakata K, Tanaka N, Yamada S, Yamamoto K, Yoshikawa J. Normal values of real-time 3-

dimensional echocardiographic parameters in a healthy Japanese population. Circ J;76:1177–81 (2012).

[39] Nagueh SF, Smiseth OA, Appleton CP, Byrd BF, Dokainish H, Edvardsen T, Flachskampf FA, Gillebert TC, Klein AL, Lancellotti P, Marino P, Oh JK, Alexandru Popescu B, Waggoner AD. Recommendations for the evaluation of left ventricular diastolic function by echocardiography: An update from the American Society of Echocardiography and the European Association of Cardiovascular Imaging. Eur Hear J – Cardiovasc Imaging;17:1321–60 (2016).

[40] Zoghbi WA, Adams D, Bonow RO, Enriquez-Sarano M, Foster E, Grayburn PA, Hahn RT, Han Y, Hung J, Lang RM, Little SH, Shah DJ, Shernan S, Thavendiranathan P, Thomas DJ, Weissman NJ. Recommendations for noninvasive evaluation of native valvular regurgitation: report from the American Society of Echocardiography developed in collaboration with the Society for Cardiovascular Magnetic Resonance. J Am Soc Echocardiogr;30:303–71 (2017).

[41] Daimon M, Akaishi M, Asanuma T, Hashimoto S, Izumi C, Iwanaga S, Kawai H, Toide H, Hayashida A, Yamada H, Murata M, Hirano Y, Suzuki K, Nakatani S, Akaishi M, Izumi C, Daimon M, Murata M, Hirano Y, Suzuki K, Yamada H. Guideline from Japanese Society of Echocardiography: 2018 focused update

incorporated into Guidance for the Management and Maintenance of Echocardiography Equipment. J Echocardiogr;16: 1-5 (2018)

[42] Bhave NM, Lang RM. Evaluation of left ventricular structure and function by three-dimensional echocardiography. Curr Opin Crit Care;19:387–96 (2013).

[43] Sonne C, Sugeng L, Watanabe N, Weinert L, Saito K, Tsukiji M, Yoshida K, Takeuchi M, Mor-Avi V, Lang RM. Age and body surface area dependency of mitral valve and papillary apparatus parameters: assessment by real-time three-dimensional echocardiograp. Eur J Echocardiogr;10:287–94 (2009).

[44] Watanabe N, Ogasawara Y, Yamaura Y, Kawamoto T, Toyota E, Akasaka T, Yoshida K. Quantitation of mitral valve tenting in ischemic mitral regurgitation by transthoracic real-time three-dimensional echocardiography. J Am Coll Cardiol;45:763–9 (2005).

[45] Xu B, Daimon M, Kawata T, Nakao T, Hirokawa M, Sawada N, Kimura K, Yamanaka Yuko, Morita H, Komuro I, Yatomi Y. Relationship between mitral leaflet size and coaptation and their associated factors in patients with normal left ventricular size and systolic function: real-time 3D echocardiographic analysis. Int Heart J; pages are in printing. (2020)

[46] Lang RM, Bierig M, Devereux RB, Flachskampf FA, Foster E, Pellikka PA,

Picard MH, Roman MJ, Seward J, Shanewise J, Solomon S, Spencer KT, Sutton MSJ, Stewart W. Recommendations for chamber quantification. Eur J Echocardiogr; 7:79–108 (2006).

[47] Yancy CW, Jessup M, Bozkurt B, Butler J, Casey DE, Drazner MH, Fonarow GC, Geraci SA, Horwich T, Januzzi J, Johnson MR, Kasper EK, Levy WC, Masoudi AF, McBride PE, McMurray JJV, Mitchell JE, Peterson PN, Riegel B, SAm F, Stevenson LW, Tang WHW, Tsai, EJ, Wilkoff BL. 2013 ACCF/AHA guideline for the management of heart failure: A report of the American College of Cardiology Foundation/American Heart Association Task Force onPractice Guidelines. J Am Coll Cardiol;62:e147–239 (2013).

[48] Olin JW, Sealove BA. Peripheral Artery Disease: Current insight into the disease and its diagnosis and management. Mayo Clin Proc;85:678–92 (2010).

[49] Levine RA, Hagége AA, Judge DP, Padala M, Dal-Bianco JP, Aikawa E, Beaudoin J, Bischoff J, Bouatia-Naji N, Bruneval P, Butcher JT, Carpentier A, Chaput M, Chester AH, Clusel C, Delling FN, Dietz HC, Dina C, Durst R, Fernandez-Friera L, Handschumacher MD, Jensen MO, Jeunemaitre XP, Marec H Le, Tourneau T Le, Markwald RR, Mérot J, Messas E, Milan DP, Neri T. Mitral valve disease-morphology and mechanisms. Nat Rev Cardiol;12:689–710

(2015).

[50] Sell S, Scully R E. Aging changes in the aortic and mitral valves.Histologic and histochemical studyies,, with observations on the pathogenesis of calcific aortic stenosis and calcification of the mitral annulus. Am J Pathol;46:345–65 (1965).

[51] Filip DA, Radu A, Simionescu M. Interstitial cells of the heart valves possess characteristics similar to smooth muscle cells. Circ Res;59:310–20 (1986).

[52] Grande-Allen KJ, Calabro A, Gupta V, Wight TN, Hascall VC, Vesely I. Glycosaminoglycans and proteoglycans in normal mitral valve leaflets and chordae: association with regions of tensile and compressive loading. Glycobiology; 14:621–33 (2004).

[53] Nordrum IS, Skallerud B. Smooth muscle in the human mitral valve: extent and implications for dynamic modelling. APMIS;120:484–94 (2012).

[54] Weiner RB, Deluca JR, Wang F, Lin J, Wasfy MM, Berkstresser B, Stöhr E, Shave R, Lewis GD, Hutter AM, Picard MH, Baggish AL. Exercise-induced left ventricular remodeling among competitive athletes: a phasic phenomenon. Circ Cardiovasc Imaging; 8: e003651 (2015).

[55] London GM. Left ventricular alterations and end-stage renal disease. Nephrol Dial Transplant;17 Suppl 1:29–36 (2002).

[56] Beltran A. Arterial compliance abnormalities in isolated systolic hypertension. Am J Hypertens;14:1007–11, (2001).

[57] Slotwiner DJ, Devereux RB, Schwartz JE, Pickering TG, de Simone G, Roman MJ. Relation of age to left ventricular function and systemic hemodynamics in uncomplicated mild hypertension. Hypertension; 37:1404–9 (2001).

[58] Franklin SS, Khan SA, Wong ND, Larson MG, Levy D. Is pulse pressure useful in predicting risk for coronary heart disease? The Framingham Heart Study. Circulation;100:354–60 (1999).

[59] Ogawa A, Shimizu K, Nakagami T, Maruoka H, Shirai K. Physical function and cardio-ankle vascular index in elderly heart failure patients. Int Heart J;61:769–75 (2020).

[60] Shirai K, Utino J, Otsuka K, Takata M. A novel blood pressure-independent arterial wall stiffness parameter; cardio-ankle vascular index (CAVI). J Atheroscler Thromb;13:101–7 (2006).

[61] Rabkin E, Aikawa M, Stone JR, Fukumoto Y, Libby P, Schoen FJ. Activated interstitial myofibroblasts express catabolic enzymes and mediate matrix remodeling in myxomatous heart valves. Circulation;104:2525–32 (2001).

[62] Thubrikar MJ, Deck JD, Aouad J, Chen JM. Intramural stress as a causative

factor in atherosclerotic lesions of the aortic valve. Atherosclerosis;55:299–311 (1985).

[63] Roberts WC. The senile cardiac calcification syndrome. Am J Cardiol;58:572–4 (1986).

[64] Wit AL, Fenoglio JJ, Hordof AJ, Reemtsma K. Ultrastructure and transmembrane potentials of cardiac muscle in the human anterior mitral valve leaflet. Circulation;59:1284–92 (1979).

[65] Wit AL, Fenoglio JJ, Wagner BM, Bassett AL. Electrophysiological properties of cardiac muscle in the anterior mitral valve leaflet and the adjacent atrium in the dog. Possible implications for the genesis of atrial dysrhythmias. Circ Res; 32:731–45 (1973).

[66] Fenoglio JJ, Tuan-Duc-Pham, Wit AL, Bassett AL, Wagner BM. Canine mitral complex. Ultrastructure and electromechanical properties. Circ Res; 31:417–30 (1972).

[67] Swanson JC, Davis LR, Arata K, Briones EP, Bothe W, Itoh A, Ingels NB, Miller DC. Characterization of mitral valve anterior leaflet perfusion patterns. J Heart Valve Dis;18:488–95 (2009).

[68] Ranganathan N, Lam JH, Wigle ED, Silver MD. Morphology of the human

mitral valve. II. The value leaflets. Circulation;41:459–67 (1970).